https://doi.org/10.5194/egusphere-2026-3809
Preprint. Discussion started: 8 July 2026

An Underappreciated Aqueous Pathway for Particle Oxidative Potential (OP): Mechanistic Insights into OP-Relevant Products from α-Dicarbonyl and Reduced Nitrogen Reactions

Yulong Pang[1], Fobang Liu[1,*], Yujing Wang[1], Xin Zhang[2], Xu Yang[1], Yanan Wang[1], Chi He[1], Yuemei Han[2,*], Theodora Nah[3]

[1]Department of Environmental Science and Engineering, School of Energy and Power Engineering, Xi'an Jiaotong University, Xi'an 710049, China

[2]Key Laboratory of Aerosol Chemistry and Physics, State Key Laboratory of Loess Science, Institute of Earth Environment, Chinese Academy of Sciences, Xi'an 710061, China

[3]School of Energy and Environment and State Key Laboratory of Marine Environmental Health, City University of Hong Kong, Hong Kong SAR 999077, China

[*]Corresponding author: Fobang Liu (fobang.liu@xjtu.edu.cn); Yuemei Han (yuemei.han@ieecas.cn)

Abstract

Aqueous-phase reactions between α-dicarbonyls and reduced nitrogen species represent an understudied pathway generating secondary organic aerosols that exhibit oxidative potential (OP). In this study, we investigated the OP of products formed from methylglyoxal (MG) or glyoxal (GX) reacting with ammonium sulfate (AS) or glycine (Gly) under varying pH (3–7) and reaction times (4–144 h). OP was quantified using dithiothreitol (DTT) depletion and hydroxyl radical (•OH) production assays, while molecular composition was characterized using high-resolution mass spectrometry and nuclear magnetic resonance spectroscopy. The results demonstrate that OP is strongly dependent on precursor identity, pH, and reaction time. Products from the MG+Gly system consistently exhibit the highest OP^{DTT} and OP^{OH}. Molecular analysis indicates that CHO species, including conjugated carbonyls and quinones, are primarily responsible for DTT activity, whereas N-heterocycles with unprotonated N-bases drive •OH formation. Electron-withdrawing substituents adjacent to the unprotonated N atoms enhance electron-transfer capability, thereby increasing

https://doi.org/10.5194/egusphere-2026-3809
Preprint. Discussion started: 8 July 2026

the ability of N-heterocycles to generate •OH. N-heterocycles also act synergistically with quinone-like species to promote DTT oxidation, highlighting their dual role in modulating OP. Collectively, these findings reveal that aqueous reactions between α-dicarbonyls and reduced nitrogen species can produce secondary organic aerosols with substantial oxidative capacity, which may contribute to oxidative stress and cause adverse health effects. This work advances mechanistic understanding of aerosol OP and emphasizes the importance of considering aqueous-phase chemistry when evaluating the health-relevant oxidative properties of ambient particulate matter.

1. Introduction

Exposure to fine particulate matter ($PM_{2.5}$) has been associated with multiple diseases and millions of premature deaths worldwide each year (Cohen et al., 2017; Zhang et al., 2025; Burnett et al., 2018; Lelieveld et al., 2015). Despite extensive epidemiological evidence for these associations, the specific physicochemical properties of $PM_{2.5}$ that drive its toxicity remain incompletely understood. One of the most widely proposed mechanisms is oxidative stress, which arises from excessive production of reactive oxygen species (ROS) that overwhelm cellular antioxidant defenses and trigger downstream inflammatory and cytotoxic responses (Saffari et al., 2014; Crobeddu et al., 2017; Fan et al., 2019). To capture the redox activity of PM constituents, the oxidative potential (OP), defined as the capacity of PM constituents to catalytically generate ROS, has emerged as an important metric for identifying redox-active PM components and evaluating PM toxicity (Li et al., 2003; He and Zhang, 2022; Bates et al., 2019). Multiple studies have shown that OP is more strongly associated with specific health endpoints than $PM_{2.5}$ mass concentration, suggesting its greater health relevance (Yang et al., 2016; Salana et al., 2024; Abrams et al., 2017; Bates et al., 2015). However, some studies have reported weak or no associations between OP and health outcomes, which may reflect the dependence of these linkages on particle composition and OP assay type (Shen et al., 2022; Atkinson et al., 2016; Strak et al., 2012).

https://doi.org/10.5194/egusphere-2026-3809
Preprint. Discussion started: 8 July 2026

$PM_{2.5}$ is a complex mixture containing inorganic ions, metals, black carbon, and organics. Among these components, transition metals, black carbon, and certain organic species (e.g., quinones and humic-like substances) have been identified as important contributors to OP (Liu et al., 2024; Charrier and Anastasio, 2012; Verma et al., 2015). The research progress of PM OP can be found in recent review articles (Bates et al., 2019; He and Zhang, 2022). Transition metals such as Fe, Cu, and Mn can catalyze Fenton-like reactions to generate ROS (Charrier and Anastasio, 2015; Lakey et al., 2016), while black carbon can act as both a carrier and an active surface for redox reactions (Li et al., 2019; Liu and Chan, 2022). In contrast, organic aerosol (OA) represents the most chemically diverse and dynamic fraction of $PM_{2.5}$, consisting of thousands of individual compounds from primary emissions and secondary formation processes. Despite its abundance (i.e., constituting 20–90% of fine PM) (Jimenez et al., 2009; Ng et al., 2010), the contribution of OA to OP remains poorly constrained, owing to its extreme molecular complexity and various sources and formation pathways.

Secondary organic aerosol (SOA) constitutes a major fraction of OA and exhibits substantial variability in chemical composition, oxidation state, and redox reactivity depending on its precursors and formation mechanisms (Liu et al., 2022; Liu et al., 2023; Huang et al., 2025). The OP of SOA formed through gas-phase photochemical oxidation has been widely investigated in both laboratory and field studies (Liu et al., 2024; Wang et al., 2018; Tuet et al., 2017; Daellenbach et al., 2020). Results consistently show that the redox activity of SOA depends strongly on precursor identity and oxidation conditions. For instance, SOA derived from polyaromatic hydrocarbons, such as naphthalene and phenanthrene, typically exhibits higher OP than that from biogenic precursors like isoprene or α-pinene, possibly due to the formation of quinone-like and polyaromatic structures with redox-active functional groups (Wang et al., 2018; Tuet et al., 2017). Furthermore, atmospheric aging processes can alter SOA OP, with the effects of whether enhancement or suppression, depending on the duration and condition of aging (Wong et al., 2019; Georgopoulou et al., 2025). These

https://doi.org/10.5194/egusphere-2026-3809
Preprint. Discussion started: 8 July 2026

findings highlight that the redox behavior of SOA is highly dynamic and closely linked to its chemical evolution in the atmosphere.

In contrast, much less attention has been given to aqueous-phase reactions, which represent an important yet less constrained route for SOA formation, particularly under atmospheric aqueous processing, or high-humidity conditions (Lai et al., 2025; Lei et al., 2025). For example, aqueous production of SOA from fossil fuel emissions was found to be a dominant mechanism for SOA formation during winter haze episodes in Beijing (Wang et al., 2021). Aqueous reactions between α-dicarbonyls (e.g., methylglyoxal, glyoxal) and reduced nitrogen species (e.g., glycine, ammonium) represent a significant aqueous SOA formation pathway (Hodzic et al., 2016; De Haan, 2018). These reactions mainly yield low-volatility nitrogen-containing compounds and are a key source of secondary brown carbon (BrC, a detailed summary of these secondary BrC can refer to De Haan (2018) and Hems et al. (2021) and references therein) (Xiao et al., 2025). The resulting light-absorbing chromophores and their optical properties are strongly influenced by the identity of the precursors, solution pH, and reaction duration. Notably, correlations have been observed between PM OP and its light absorption, suggesting that BrC chromophores may possess intrinsic redox activity and contribute to oxidative stress (Kuang et al., 2020; Chen et al., 2019b). However, the oxidative behavior of products formed from reactions between α-dicarbonyl and reduced nitrogen species remains largely unexplored, hindering our understanding of their potential toxicological relevance and atmospheric implications. In particular, several key scientific questions remain unresolved: 1) how reaction conditions such as pH and reaction time regulate the formation of OP-active species; 2) whether BrC chromophores formed in these systems contribute to OP; and 3) which specific molecular features control the OP of these products, and what are the underlying mechanisms.

To address this gap, we systematically investigated the OP of these aqueous reaction products using model systems of methylglyoxal or glyoxal with glycine or ammonium sulfate under a range of pH conditions (3–7) and reaction times

https://doi.org/10.5194/egusphere-2026-3809
Preprint. Discussion started: 8 July 2026

(4–144 h). Glyoxal is the most abundant carbonyl compound in atmospheric aerosols, followed by methylglyoxal, while ammonium sulfate and glycine are ubiquitous components of atmospheric aerosols worldwide (Trainic et al., 2012; De Haan, 2018; Mitsuishi et al., 2018; Kawamura et al., 2013). Two complementary assays were employed to measure OP: the dithiothreitol (DTT) assay, which reflects the electron-transfer reactivity linked to superoxide and hydrogen peroxide formation, and the hydroxyl radical (•OH) assay, which captures hydroxyl radical-generating capacity (Fang et al., 2019; Yang et al., 2024b). To elucidate the molecular basis of OP, the optical properties and molecular information of the reaction products were characterized using UV-Vis, nuclear magnetic resonance (NMR) spectroscopy, and high-resolution mass spectrometry analyses. The integrated results reveal distinct pH- and time-dependent evolution of OP, identify molecular features associated with DTT and •OH reactivities, and provide mechanistic insights into the formation of products with oxidative capacity in atmospheric aqueous systems.

2. Materials and Methods

2.1 Reagents

Ammonium sulfate (AS, ≥99%), glycine (Gly, ≥98%), dithiothreitol (DTT, ≥99%), 5,5'-dithiobis-(2-nitrobenzoic acid) (DTNB, ≥99%), and L-ascorbic acid (AA, ≥99%) were purchased from Sigma-Aldrich. Glyoxal (GX, 39 wt% aqueous solution), 2-hydroxyterephthalic acid (2-OHTA, ≥99%), and dimethyl sulfoxide (DMSO, ≥99%) were obtained from Tokyo Chemical Industry. Disodium terephthalate (TPT, ≥99%) was acquired from Thermo Scientific. Methylglyoxal (MG, 40 wt% aqueous solution) and ethylenediaminetetraacetic acid (EDTA, ≥99%) were obtained from Aladdin. Deuterium oxide (D_2O, 99.9%) was supplied by Adamas. Buffer reagents included Tris-HCl (pH 7.0–9.0, Beyotime) and phosphate-buffered saline (PBS, pH 7.4, Biosharp). Sodium hydroxide (NaOH, ≥97%) was purchased from Macklin, and hydrochloric acid (HCl, 36 wt% aqueous solution) from HUSHI.

https://doi.org/10.5194/egusphere-2026-3809
Preprint. Discussion started: 8 July 2026

2.2 Aqueous aerosol mimicry experiments

Stock solutions (2 M) of MG, GX, AS, and Gly were prepared in ultrapure water. Four reaction systems were investigated: GX+AS, GX+Gly, MG+AS, and MG+Gly. The reactions were conducted in a bulk aqueous-phase batch reactor to simulate atmospheric aqueous processing. Briefly, stock solutions were mixed in glass vials to obtain initial concentrations of 0.5 M GX (or MG) and 0.5 M AS (or Gly) (Powelson et al., 2013; Rodriguez et al., 2017; Hawkins et al., 2016). The pH of each reaction system was adjusted to 3.0, 5.0, 6.0, and 7.0 using HCl or NaOH, and measured with a pH sensor (INESA) (Kampf et al., 2016). These pH values are within the range observed in real atmospheric environments (e.g., aerosol particles, cloud, and fog droplets) (Tilgner et al., 2021; Pye et al., 2020). The reaction mixtures were reacted in the dark at room temperature to avoid photochemical effects. At predetermined time intervals (4, 24, 48, 96, and 144 h, 144 h indicates the upper limit of the atmospheric lifetime of an SOA particle), aliquots were withdrawn using pipettes for OP measurements or chemical analysis. A schematic diagram of the experimental configuration is provided in Figure S1. This bulk-phase approach is widely used to investigate aqueous SOA formation mechanisms and their associated physicochemical properties (Yang et al., 2024a; Yang et al., 2023). The reactant concentrations employed here represent an intermediate case between highly concentrated SOA particles and dilute cloud droplets (Kampf et al., 2016). Such conditions are commonly adopted in laboratory studies to accelerate reaction kinetics and facilitate the detection and characterization of reaction products within experimentally feasible timescales (Yang et al., 2024a; Ervens et al., 2011; De Haan et al., 2009). Nevertheless, this simplified system does not fully capture the complexity of real atmospheric processes such as interfacial reactions, photochemistry, and dynamic gas-particle mass transfer, which are often simulated using flow reactors or chamber systems (Wang et al., 2018; Campbell et al., 2023). All aqueous aerosol mimicry experiments and subsequent measurements were conducted in duplicates.

2.3 Oxidative potential measurements

https://doi.org/10.5194/egusphere-2026-3809
Preprint. Discussion started: 8 July 2026

The OP of the products was measured using two assays: the DTT depletion assay and •OH production assay. In the DTT assay, 100 μM DTT in phosphate buffer was incubated with samples at 37 °C for 40 min. The remaining DTT was quantified by its reaction with DTNB, yielding ultraviolet-detectable 2-nitro-5-thiobenzoic acid. In the •OH production assay, 10 mM TPT in phosphate buffer was incubated with samples and 200 μM ascorbic acid at 37°C for 1 h. TPT was used as a probe to measure •OH radical formation, a method that has been well established and widely used in previous studies (Xiong et al., 2017; Li et al., 2018). At pH 7.4, TPT reacted with •OH to form stable and highly fluorescent hydroxyterephthalic acid (2-OHTA). The production rate of •OH was calculated based on the produced 2-OHTA, as the formation of 2-OHTA is proportional to the generation of •OH (Yang et al., 2024b). To minimize the loss of short-lived or volatile species, OP measurements were performed immediately after sampling at each predetermined time interval. Nevertheless, some labile compounds may still degrade or evaporate within minutes during handling, which could underestimate the measured OP (Campbell et al., 2025). A detailed description of the DTT and •OH protocols can be found in the Supporting Information (Text S1).

2.4 Light absorption measurements

The UV-Vis light absorption spectra of the samples were analyzed using a microplate reader (SuPerMax3000FA, Shanghai Flash Spectrum). For analysis, 200 μL of each sample was loaded into a 96-well plate. The instrument was operated with a 1 nm slit width over a wavelength range of 200–700 nm. Due to differences in overall absorbance, two different dilution ratios were prepared and analyzed: 1:80 for the glycine system and 1:20 for the ammonium sulfate system. The absorption coefficient at 365 nm (Abs_{365}) is used to represent BrC absorption (Huang et al., 2018).

2.5 Nuclear magnetic resonance measurements

https://doi.org/10.5194/egusphere-2026-3809
Preprint. Discussion started: 8 July 2026

The product distributions under different conditions were characterized by ^{1}H-NMR spectroscopy to determine the proportions of four distinct hydrogen environments. Concurrently, the concentration changes of key reactants were determined quantitatively by an internal standard method to monitor the reaction kinetics. The accuracy and sensitivity of this approach rely on the clear spectral resolution between the internal standard and target compounds, as well as the linear relationship between the integral peak area and concentration. To ensure system stability and data reliability, all samples were prepared with a fixed solvent ratio (DMSO: 10 μL, D_2O: 100 μL, sample: 500 μL). Before mixing, the pH of the samples was adjusted to 3.0 using HCl. D_2O served as the lock solvent, and DMSO (δ 2.50 ppm) was used as the internal standard. Spectra were acquired on a Bruker 400 MHz NMR spectrometer. The concentrations of target compounds were calculated by comparing the integral areas of their characteristic peaks with that of the internal standard peak (Tang et al., 2022; Yu et al., 2011). Peak area integration was performed using MestReNova software. The NMR signals of reactant and product species were monitored as detailed in Table S1.

2.6 UHPLC–HRMS/MS Analysis

The products were analyzed using a Vanquish Flex ultrahigh-performance liquid chromatograph coupled with a Q-Exactive Orbitrap high-resolution mass spectrometer (UHPLC–HRMS, Thermo Scientific Inc.), following procedures described previously (Yang et al., 2023). Chromatographic separation was achieved on a Thermo Hypersil Gold C_{18} column (100×2.1 mm, 1.9 μm particle size). A binary gradient elution at 0.25 mL/min was used, with mobile phase A consisting of water containing 0.5% formic acid and mobile phase B consisting of acetonitrile with 0.5% formic acid. The gradient elution program was as follows: 5% mobile phase B (0–3 min), ramped to 40% (3–10 min), and further ramped to 90% (10–30 min), held at 90% (30–35 min) mobile phase B, then returned to 5% mobile phase B (35–36 min), and re-equilibrated at 5% B (36–40 min). The sample injection volume was 5 μL. Mass spectrometric analysis was performed with an electrospray ionization source in positive mode (ESI+). The parameters were as follows: sheath

https://doi.org/10.5194/egusphere-2026-3809
Preprint. Discussion started: 8 July 2026

gas flow at 40 units, auxiliary gas flow at 10 units, capillary temperature set at 320 °C, and spray voltage at 3.2 kV. Besides, the reaction mixtures were also analyzed in Full MS/dd-MS2 mode. Mass spectra were acquired over m/z 65–800 at a resolution of 70,000 (m/z 200) (Yang et al., 2023). The raw UHPLC–HRMS/MS data were visualized using Xcalibur software and processed using the open-source software MZmine 4.5 (http://mzmine.github.io/). Low-intensity signals were filtered out by applying a minimum intensity threshold of 10^5 (Pluskal et al., 2010; Siemens et al., 2022), and chromatograms were generated with a mass tolerance of 2 ppm. Molecular structures were subsequently identified from MS/MS fragmentation trees using SIRIUS 6.1 software, a high-performance tool for small-molecule identification that has been widely applied to structural annotation in complex atmospheric organic aerosols (Dührkop et al., 2019; Ditto et al., 2020). Note that, consistent with previous studies (Wang et al., 2017; Laskin et al., 2015), ESI+ was used in this study as it effectively detects most nitrogen-containing compounds. However, some species, particularly those with acidic functional groups, may ionize more efficiently in negative mode (ESI-). Future work could include complementary analyses (e.g., ESI-) to achieve a more comprehensive molecular characterization.

3. Results and discussion

3.1 pH- and time-dependent oxidative potential of reaction products

The products formed in the four reaction systems exhibit distinct OP, as illustrated in Figure 1, which shows a representative result for systems generated at pH 5 over 48 hours. Among them, MG+Gly displays both substantially higher OP^{DTT} and OP^{OH} than the standard references (1 μM 1,4-naphthoquinone (1,4-NQ) for the DTT assay and 100 μM Cu^{2+} for the •OH assay) (Yue et al., 2018; Lin and Yu, 2020). In contrast, MG+AS shows negligible OP^{DTT} and OP^{OH} compared with the standards. Interestingly, both GX+Gly and GX+AS systems exhibit pronounced OP^{OH} but negligible OP^{DTT}. Previous work suggested that OP^{DTT} is a good indicator of the production of superoxide anion ($O_2^{-\bullet}$) and hydrogen peroxide (H_2O_2), but does not capture •OH generation (Fang et al., 2019). Thus, the products from

https://doi.org/10.5194/egusphere-2026-3809
Preprint. Discussion started: 8 July 2026

GX+Gly/AS may preferentially promote •OH generation rather than $O_2^{-\bullet}$ and/or H_2O_2 formation. Note that the potential interference by the reactants and trace metals is expected to be minimal, as all individual reactants prepared using the same ultrapure water exhibit negligible OP. Therefore, these results indicate products with high OP can be formed in the reactions of α-dicarbonyl with ammonium or amine.

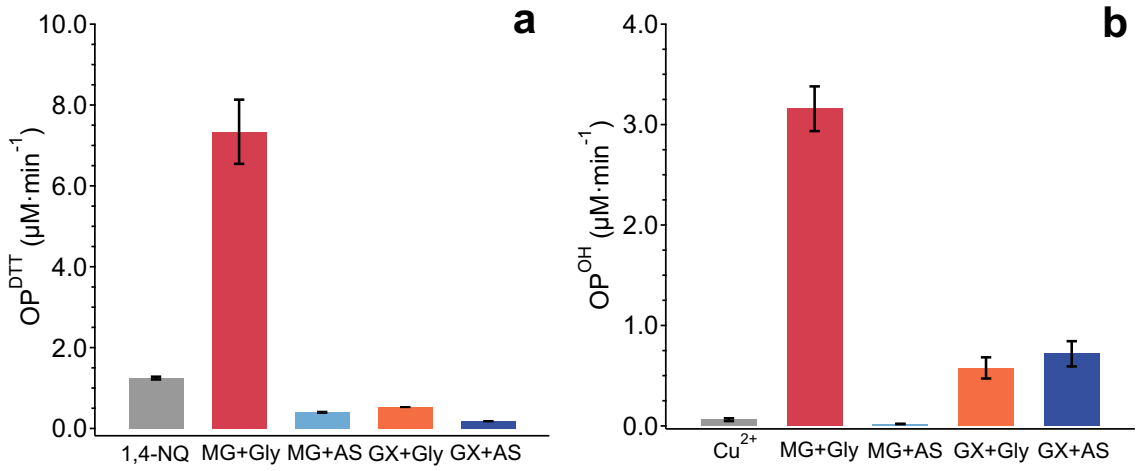

Figure 1. Comparison of oxidative potential (OP) between the standard reference and the four reaction systems after 48-h reaction at pH 5.0. (a) OP^{DTT} of 1,4-naphthoquinone (1,4-NQ, 1 μM) and the four reaction systems. (b) OP^{OH} of 100 μM Cu^{2+} standard and the four reaction systems.

To further explore the OP of the reaction products, the OP of the products formed from the four reaction systems under different pH conditions (3, 5, 6, and 7) over a wide range of reaction time (4–144 h) was measured. Figure 2 shows the temporal evolution of OP^{DTT} for products formed in the four reaction systems under different pH conditions. As mentioned above, only MG+Gly exhibits a notable OP^{DTT} at pH 5. In contrast, OP^{DTT} values remain close to zero at pH 3 for all the reaction systems throughout the reaction period. This is likely due to the suppression of reactions between α-dicarbonyls and ammonium or amine species under acidic conditions (pH < 5), as demonstrated by previous work (Ervens and Volkamer, 2010). A strong pH dependence of OP^{DTT} is observed in the MG+Gly system (Figure 2a),

https://doi.org/10.5194/egusphere-2026-3809
Preprint. Discussion started: 8 July 2026

with values increasing markedly from pH 5 to 7 (except at the reaction time of 144 h). This finding suggests that less acidic conditions favor the formation of more redox-active products, or products with higher intrinsic redox activity (Yang et al., 2024a). Similarly, a pH-dependent trend is also observed in MG+AS (Figure 2b), where higher OP^{DTT} values are determined at pH 6 and 7, although these remain one to two orders of magnitude lower than those in the MG+Gly system. This strong pH-dependent behavior has also been observed for the BrC formation in these α-dicarbonyl and reduced nitrogen reaction systems (Yang et al., 2024a; Sedehi et al., 2013). In contrast, negligible OP^{DTT} is consistently observed for GX+Gly and GX+AS systems across all pH conditions (Figures 2c and 2d), indicating that their products exhibit no measurable OP^{DTT}.

The temporal evolution of OP^{DTT} exhibits an overall increasing trend with reaction time, but the pattern differs among pH conditions, particularly in MG+Gly (Figure 2a). At pH 7, the OP^{DTT} increases rapidly during the first 48 h, followed by a slower rise, suggesting that highly redox-active products form quickly under neutral conditions, after which product stabilization or depletion of reactive precursors limits further increases (Sedehi et al., 2013). In contrast, at pH 5–6, OP^{DTT} increases steadily during the initial 48 h and then accelerates, indicating that product formation is initially slower under mildly acidic conditions but intensifies as reaction intermediates accumulate (Pripis-Nicolau et al., 2000; Tessier et al., 2003).

https://doi.org/10.5194/egusphere-2026-3809
Preprint. Discussion started: 8 July 2026

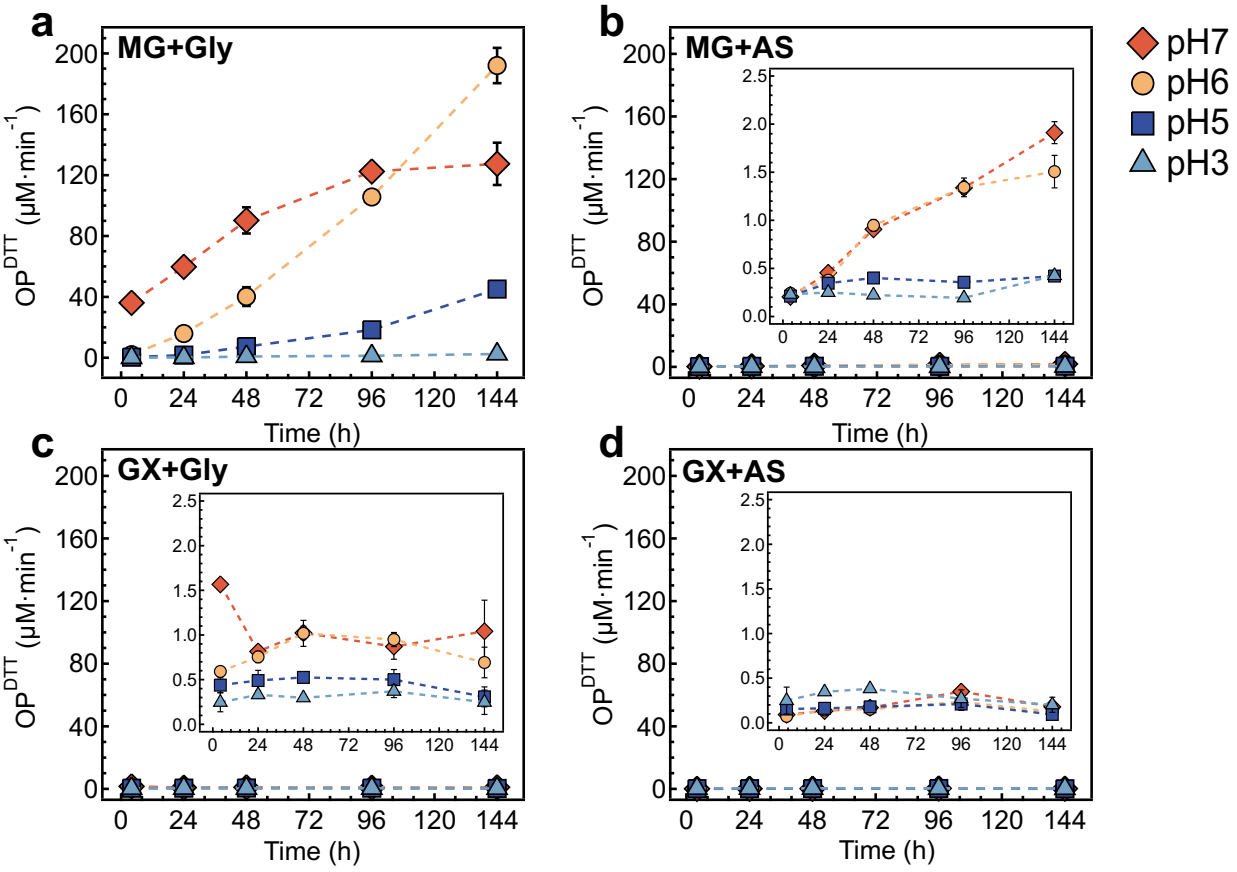

Figure 2. The temporal evolution of OP^{DTT} for products in the four reaction systems under different pH conditions: (a) methylglyoxal with glycine (MG+Gly), (b) methylglyoxal with ammonium sulfate (MG+AS), (c) glyoxal with glycine (GX+Gly), and (d) glyoxal with ammonium sulfate (GX+AS). The insets show magnified views of the OP^{DTT} in the corresponding panels.

In terms of OP^{OH}, the products in all four reaction systems exhibit clear pH- and time-dependent patterns (Figure 3), but the behaviors vary among systems and also differ from those of OP^{DTT}. First, all four reaction systems produce considerable OP^{OH} at pH 5–7, except for MG+AS at pH 5. These results indicate that the products formed in all four systems under mildly acidic to neutral conditions possess a consistent capacity to generate •OH. In addition, the OP^{OH} values increase with pH in MG+Gly (Figure 3a) and GX+AS (Figure 3d) systems, whereas they remain comparable in MG+AS (pH 6–7, Figure 3b) and GX+Gly (pH 5–7, Figure 3c). Among the four systems, MG+Gly yields the highest

https://doi.org/10.5194/egusphere-2026-3809
Preprint. Discussion started: 8 July 2026

OP^{OH} values, followed by GX+AS, while MG+AS and GX+Gly exhibit substantially lower values. These results indicate that the products in MG+Gly and GX+AS systems have a stronger •OH-generating capacity that is more sensitive to pH variations, whereas those in MG+AS and GX+Gly systems form less reactive products with limited pH dependence.

The temporal evolution of OP^{OH} further reveals distinct kinetic characteristics among the four reaction systems (Figure 3). In the MG+Gly system, OP^{OH} increases rapidly during the first 48 h and then gradually approaches a plateau, implying the rapid formation of highly •OH-generating products that subsequently reach steady levels. At pH 7, however, a slight decline in OP^{OH} is observed after 144 h, likely indicating the further transformation or consumption of OH-generating products. The MG+AS system exhibits a similar time-dependent profile but with much lower OP^{OH} values, suggesting that ammonium limits the formation of •OH-generating species or stabilizes less reactive products. In contrast, the GX+Gly and GX+AS systems display a slower initial increase in OP^{OH} within the first 48 h, followed by a more pronounced rise between 48 and 96 h and eventual stabilization thereafter. These delayed responses may reflect the gradual accumulation of reactive intermediates from glyoxal oxidation, which require longer reaction time to generate •OH-active compounds. This interpretation is consistent with previous studies showing that the aqueous reactions of glyoxal with amines or ammonium proceed much more slowly than those of methylglyoxal (Sedehi et al., 2013; Yu et al., 2011).

https://doi.org/10.5194/egusphere-2026-3809
Preprint. Discussion started: 8 July 2026

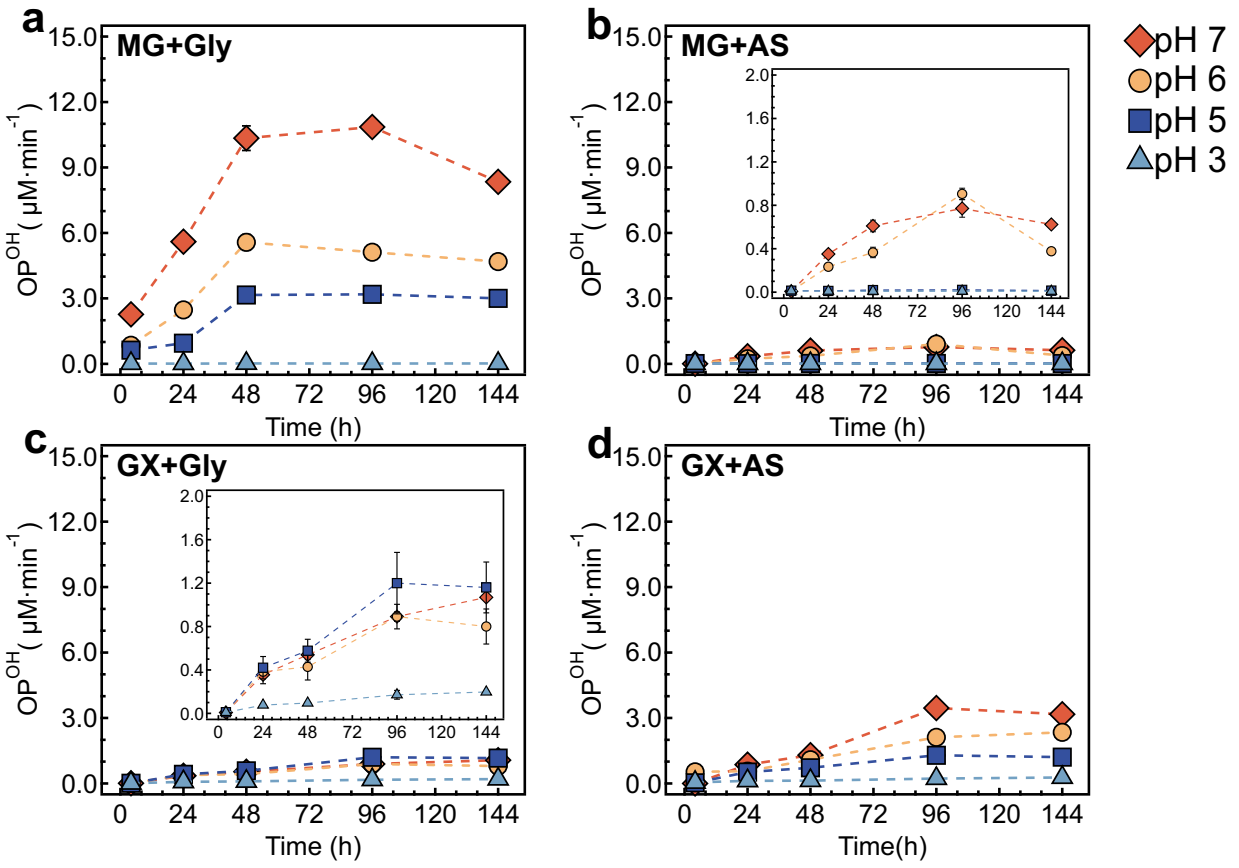

Figure 3. The temporal evolution of OP^{OH} for products in the four reaction systems under different pH conditions: (a) methylglyoxal with glycine (MG+Gly), (b) methylglyoxal with ammonium sulfate (MG+AS), (c) glyoxal with glycine (GX+Gly), and (d) glyoxal with ammonium sulfate (GX+AS). The insets show magnified views of the OP^{OH} in the corresponding panels.

Overall, both OP^{DTT} and OP^{OH} exhibit strong dependencies on precursor type, pH, and reaction time. The MG+Gly system stands out for producing the most products with oxidative capacity, as evidenced by its consistently highest OP^{DTT} and OP^{OH} among all four systems. Neutral to mildly acidic conditions (pH 5–7) appear to favor the formation of these species, while acidic conditions (pH 3) largely suppress their production (Yang et al., 2023; Ervens and Volkamer, 2010). The pronounced differences of temporal evolution between methylglyoxal- and glyoxal-based systems, as well as between ammonium- and amine-containing reactions, also highlight the critical influence of precursor chemistry and

https://doi.org/10.5194/egusphere-2026-3809
Preprint. Discussion started: 8 July 2026

nitrogen speciation on redox product formation. Collectively, these findings suggest that distinct molecular pathways govern the generation of DTT- and •OH-active species, motivating further understanding into the specific chemical compositions and mechanisms responsible for the observed OP.

3.2 Associations between oxidative potential and brown carbon

To explore the relationship between OP and BrC chromophores, we characterized the light-absorbing properties of the reaction products and linked them to the corresponding OP metrics. The light absorption spectra (200–700 nm) of the products formed in the four systems under different pH conditions and reaction times are shown in Figure S2. The observed trends are consistent with previous studies (Trainic et al., 2012; Kampf et al., 2016), although a detailed analysis of the light-absorbing properties of the products and their dependence on pH and time is beyond the scope of this work. Briefly, all systems exhibit a general increase in absorbance with both increasing pH and reaction time. In addition, glycine promotes BrC formation (indicated by enhanced absorption between 300 and 500 nm) more effectively than ammonium sulfate (Powelson et al., 2013). The absorbance is also stronger in methylglyoxal-containing systems compared to those with glyoxal (Yang et al., 2023). Therefore, the MG+Gly system exhibits the most pronounced BrC absorption characteristics among the four systems. These variations in BrC optical properties are also reflected in the distinct color of the resulting solutions (Figure S3).

To investigate whether BrC components contribute to the OP in the four reaction systems, the absorption coefficients of BrC (Abs_{365}) were correlated with OP^{DTT} (for the MG+Gly system) and OP^{OH} (for all four systems) at pH 6–7, where OP values are the highest. The resulting Spearman coefficients (r) are presented in Figure 4, and the corresponding scatter plots are shown in Figures S4 and S5. In the MG+Gly system, Abs_{365} is significantly correlated with both OP^{DTT} ($r = 0.78$, $p < 0.01$) and OP^{OH} ($r = 0.84$, $p < 0.01$). These correlations suggest that BrC components are strongly associated with products contributing to OP^{DTT} and OP^{OH}. Consistently, the other three systems also show

https://doi.org/10.5194/egusphere-2026-3809
Preprint. Discussion started: 8 July 2026

significant correlations between Abs_{365} and OP^{OH}. In addition, while some OP values at pH 5 are relatively low and may introduce additional variability, we also performed Spearman correlation analysis across pH 5-7. The results indicate significant correlations between Abs_{365} and OP (Figure S6), confirming that BrC components are associated with oxidative potential across a broader pH range, albeit with minor differences compared to pH 6–7.

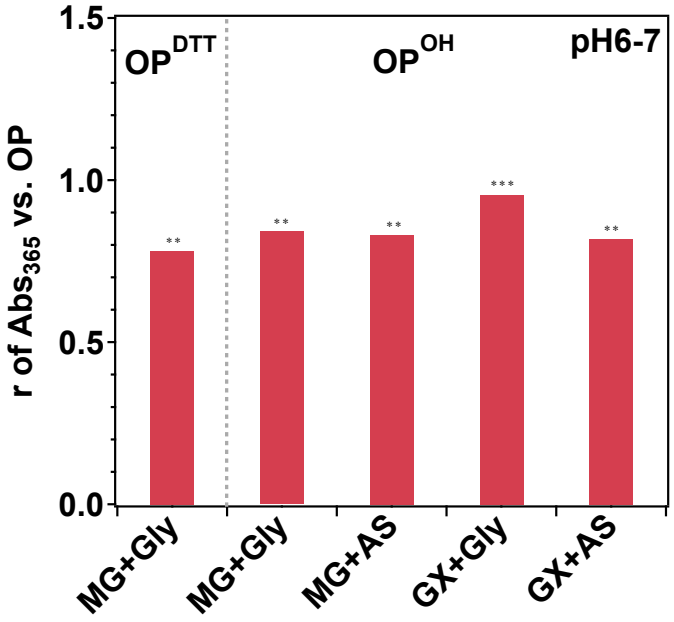

Figure 4. Spearman correlation (represented by the Spearman correlation coefficient, r) between the BrC absorption coefficient (Abs_{365}) and OP metrics (OP^{DTT} for the MG+Gly system; OP^{OH} for all four reaction systems) under pH 6–7 conditions. Statistically significant differences were determined with a t-test using a 95% confidence interval (*, **, and *** indicate $p < 0.05$, $p < 0.01$, and $p < 0.001$, respectively).

Our results indicate that BrC components are likely to participate in oxidative processes that consume DTT and generate •OH. However, their specific roles in contributing to the oxidative capacity in these systems need to be further elucidated. The contribution can be direct or indirect. For example, BrC components may act as adjuvants that facilitate electron-transfer processes (Kipp et al., 2004; Dou et al., 2015). Although previous studies have suggested that BrC formed in these four systems mainly consists of nitrogen-containing compounds (e.g., imidazoles, pyrroles) (Haan et

https://doi.org/10.5194/egusphere-2026-3809
Preprint. Discussion started: 8 July 2026

al., 2009; De Haan et al., 2018), the specific nitrogen-containing species responsible for the OP (OP^{DTT} and OP^{OH}) remain ambiguous. Hence, it is essential to identify the molecular structures of the BrC species that contribute to OP^{DTT} and OP^{OH}, in order to gain a more mechanistic understanding of the formation of products with oxidative capacity in these reaction systems.

3.3 Molecular characteristics and mechanisms underlying product oxidative potential

To elucidate the molecular characteristics and mechanisms underlying the observed OP, we conducted detailed molecular analyses of the reaction products using UHPLC–HRMS/MS and NMR techniques. While the NMR technique was used to analyze all samples, only a subset was selected for UHPLC–HRMS/MS analysis, representing key conditions with distinct OP values and variations.

OP^{DTT}. Figure 5a shows the peak area-weighted fraction of molecular composition for the four reaction systems under identical conditions (pH 7, 96 h). Nitrogen-containing compounds are the dominant species in all reaction systems, which is consistent with previous studies (Yang et al., 2023; Tang et al., 2022). Notably, the MG+Gly system, which is the only system exhibiting notable OP^{DTT}, contains a distinctly higher fraction of CHO species (10.9%, compared with <3% in the other systems). This enrichment of CHO species is consistently observed across all conditions analyzed by LC-MS/MS for the four systems (Figure S7). Therefore, the CHO species are speculated to be responsible for the notable OP^{DTT} in the MG+Gly system. To further evaluate the link between CHO species and OP^{DTT}, we compared the total signal abundance of CHO species with OP^{DTT} values across different MG+Gly conditions. The abundance of CHO species exhibits a similar trend to OP^{DTT} (Figure 5b), and correlation analysis confirms a significant relationship (R^2=0.80, p <0.05, Figure S8). These results strongly suggest that CHO species are the main contributors to the observed OP^{DTT} in the MG+Gly system.

https://doi.org/10.5194/egusphere-2026-3809
Preprint. Discussion started: 8 July 2026

To further probe how CHO species contribute to DTT oxidation, we identified the likely molecular structures of the major CHO species detected in the MG+Gly system (Figures 5c and S9). Notably, these CHO compounds share a key structural feature: ring-containing frameworks with conjugated carbonyl groups. Such conjugated systems are well-known reactive electrophiles and can readily engage in nucleophilic or conjugate-addition reactions, thereby contributing to DTT consumption (Chen et al., 2019a; Jiang and Jang, 2018; Jiang et al., 2019). For example, $C_6H_8O_3$, one of the ten most abundant CHO species formed under pH 5 and 6 (Figure S9), is identified as 2,5-dimethyl-4-hydroxy-3(2H)-furanone, featuring a furan ring adjacent to a conjugated carbonyl group, based on its assigned molecular formula with minimum mass error and its MS/MS fragmentation pattern (Figure S10a). This compound has also been reported in prior work (Wang and Ho, 2008), further supporting its formation in the MG+Gly reaction system. Additionally, several CHO species with conjugated carbonyl groups but lacking ring structures were detected (e.g., $C_6H_{10}O_4$ and $C_8H_{10}O_4$, Figures S10b and S10c). Although these molecules occur at relatively low abundance, their conjugated motifs have been shown to induce DTT consumption in previous studies (Jiang et al., 2020; Chen et al., 2019a).

https://doi.org/10.5194/egusphere-2026-3809
Preprint. Discussion started: 8 July 2026

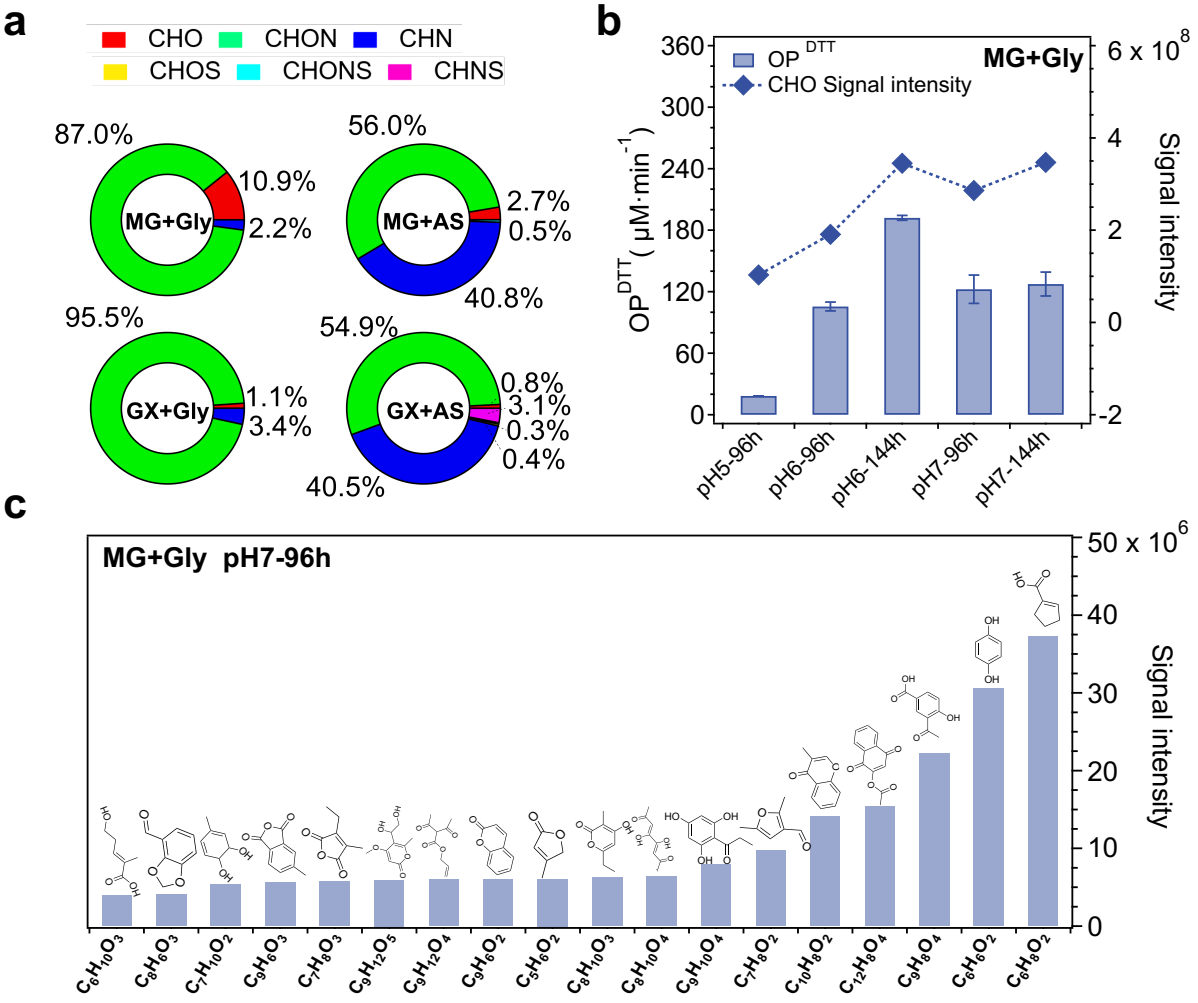

325 **Figure 5.** (a) The peak area-weighted fraction of molecular composition for the four reaction systems after 96 h of reaction under pH 7. (b) Abundance of CHO species and OP^{DTT} for the MG+Gly system under different conditions. (c) The possible molecular structures of the major CHO species detected in the MG+Gly system after 96 h of reaction under pH 7.

In addition to these conjugated carbonyl species, quinone-type compounds are an important subgroup within the

330 CHO class that may contribute to DTT consumption. For instance, $C_6H_6O_2$, another abundant CHO compound in the MG+Gly system, as shown in Figure 5c, is identified as hydroquinone (Figure S10d). Hydroquinones are known to be unstable at physiological pH and can undergo autoxidation to form semiquinone radicals and quinones (Guin et al.,

https://doi.org/10.5194/egusphere-2026-3809
Preprint. Discussion started: 8 July 2026

2011; Wei et al., 2022), both of which are well recognized as strong oxidants in the DTT assay (Twerdok et al., 1993; Dou et al., 2015). Therefore, the quinone-type compounds, although not all of them present at high abundance, can contribute substantially to OP^{DTT} in the MG+Gly system, given their high intrinsic redox activity.

Building on these structural assignments, we propose two major formation mechanisms for the identified CHO species and their corresponding DTT-reactive pathways (Figure 6). One is the conjugated carbonyl pathway (Figures 6a and 6b), where the identified CHO compounds are dominated by cyclic α,β-unsaturated carbonyl compounds. The mechanism likely begins with the hydration of methylglyoxal to form hydroxyketone intermediates, followed by enol–keto tautomerization that produces multi-hydroxy ketones. These intermediates undergo intramolecular cyclization to generate furan-like structures, which then experience proton transfer and dehydration to yield cyclic α,β-unsaturated carbonyl groups (i.e., conjugated carbonyl compounds). Such formation routes for these conjugated carbonyls have been proposed by previous studies (Wang and Ho, 2008; Kampf et al., 2016). Importantly, these conjugated structures can react with DTT through two pathways: 1) 1,4-Michael addition, in which the nucleophilic thiol group of DTT attacks the β-carbon of the α,β-unsaturated carbonyl; and 2) 1,2-nucleophilic addition, in which the thiol directly attacks the electrophilic carbonyl carbon (Chen et al., 2019a). Both reactions result in thiol addition and therefore DTT consumption, constituting a major contributor to the OP^{DTT} observed in the MG+Gly system.

The second mechanism is the quinone pathway, which forms quinone-type species through sequential carbonyl chemistry (Figures 6c and 6d). In this pathway, methylglyoxal generates hydroxyacetone and formaldehyde (via Strecker degradation with glycine), which then undergo aldol-type condensation to produce polyhydroxy-ketone intermediates (Xing and Yaylayan, 2024; De Haan et al., 2009). These intermediates dehydrate to α,β-unsaturated carbonyls, some of which tautomerize to diacetyl (Melvin et al., 2020). Condensation and dehydration of diacetyl-derived intermediates progressively extend the conjugated system, and final acid-catalyzed intramolecular cyclization

https://doi.org/10.5194/egusphere-2026-3809
Preprint. Discussion started: 8 July 2026

yields quinone-like products (Grace et al., 2020). The key intermediate products were identified and their MS/MS fragmentation patterns are shown in Figure S11, further supporting the proposed formation pathway. As discussed above, quinones readily undergo redox cycling, forming semiquinone radicals and ROS that efficiently oxidize DTT. In addition, N-heterocycles with unprotonated N-base (e.g., imidazole), although not strong oxidants themselves, can enhance electron-transfer processes by forming hydrogen-bonding complexes with quinone intermediates (Dou et al., 2015). This synergistic effect further promotes DTT oxidation, indicating that the quinone pathway may also play an important role in the OP^{DTT} observed in the MG+Gly system.

https://doi.org/10.5194/egusphere-2026-3809
Preprint. Discussion started: 8 July 2026

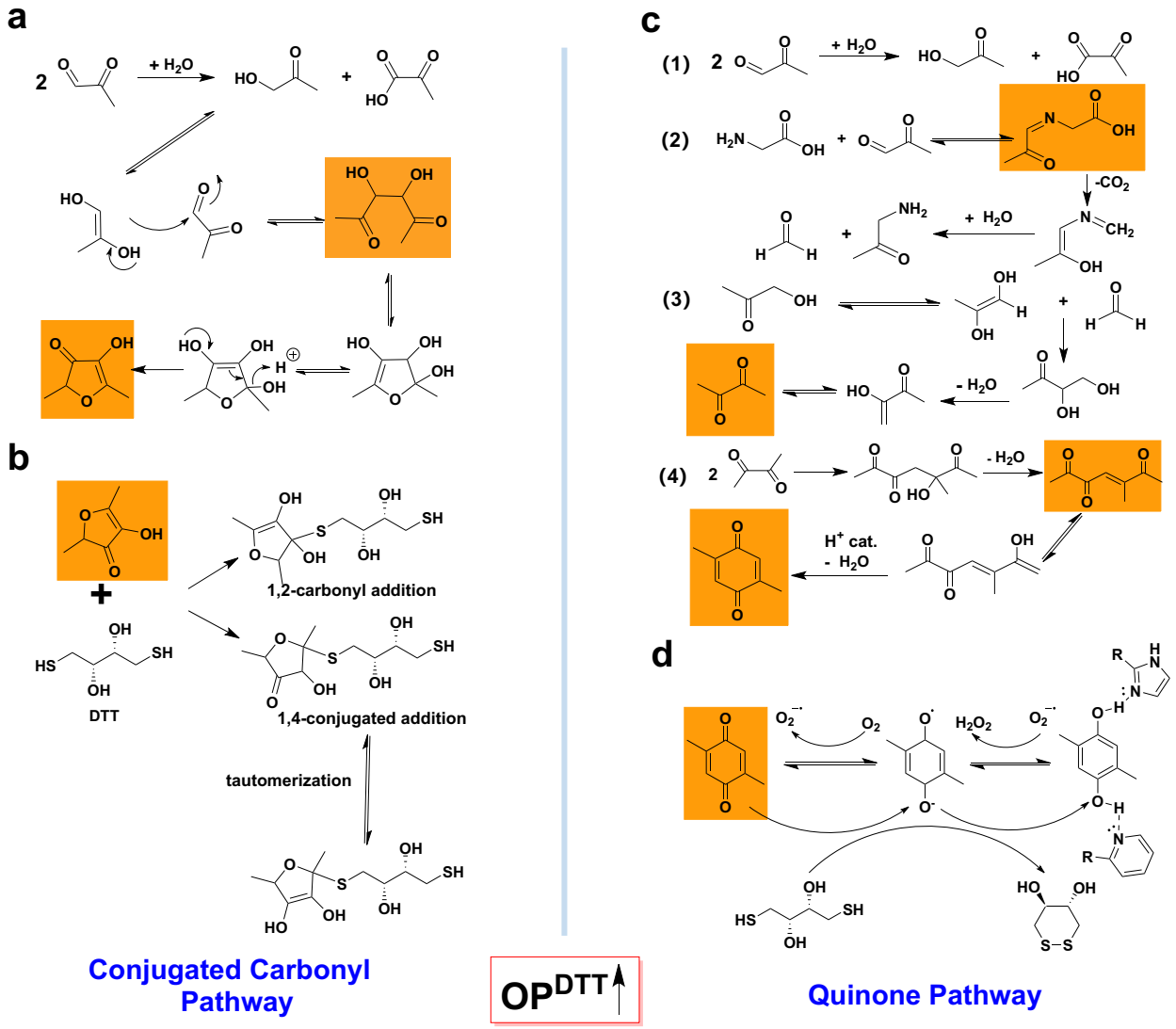

Figure 6. The proposed mechanisms for the identified CHO species and their corresponding DTT consumption pathways. (a, b): the mechanisms for forming conjugated carbonyl products (take the cyclic α,β-unsaturated carbonyl compound ($C_6H_8O_3$) as a representative) and their corresponding DTT consumption pathways; (c, d): the mechanisms for forming quinone-type compounds (take $C_8H_8O_2$) as a representative) and their DTT consumption pathway.

To further validate their contributions, OP^{DTT} was measured for representative CHO compounds. Quinone-type species exhibit substantially higher intrinsic reactivity, with 1 μM hydroquinone and 2,5-dimethyl-1,4-benzoquinone

https://doi.org/10.5194/egusphere-2026-3809
Preprint. Discussion started: 8 July 2026

yielding OP^{DTT} values of 0.11 and 0.28 μM min^{-1} (Figure S12a), respectively, whereas 100 μM conjugated carbonyl compounds produce comparable OP^{DTT} (~0.29 μM min^{-1}, Figure S12b). Given the higher abundance of conjugated carbonyls than quinones, these results indicate that both quinones and conjugated carbonyls are capable of driving DTT consumption and contribute to the observed OP^{DTT} in the MG+Gly system.

OP^{OH}. Previous studies have elucidated the mechanisms of metal-mediated •OH formation in the presence of a reductant such as ascorbic acid. In this process, redox-active metals catalyze electron transfer from ascorbic acid to dissolved O_2, promoting the formation of H_2O_2 and subsequently •OH (Charrier and Anastasio, 2011; Vidrio et al., 2008; Lin and Yu, 2020). In addition, it has been shown that N-heterocycles with unprotonated N-base can facilitate electron-transfer reactions from organic reductants (Kipp et al., 2004). Therefore, the N-heterocyclic compounds detected in the four reaction systems are likely contributors to the observed OP^{OH} in this work. To examine this possibility, we identified all the potential N-heterocycles with unprotonated N-base from the LC-MS/MS results and compared their signal intensities with OP^{OH}. Although no clear correlation emerges when considering all the data from the four reaction systems collectively, significant correlations are observed in the MG/GX+Gly systems (Figure 7a). These results suggest that N-heterocycles with unprotonated N-base in the four reaction systems exhibit varying abilities in promoting •OH formation, besides differences in their abundances.

https://doi.org/10.5194/egusphere-2026-3809
Preprint. Discussion started: 8 July 2026

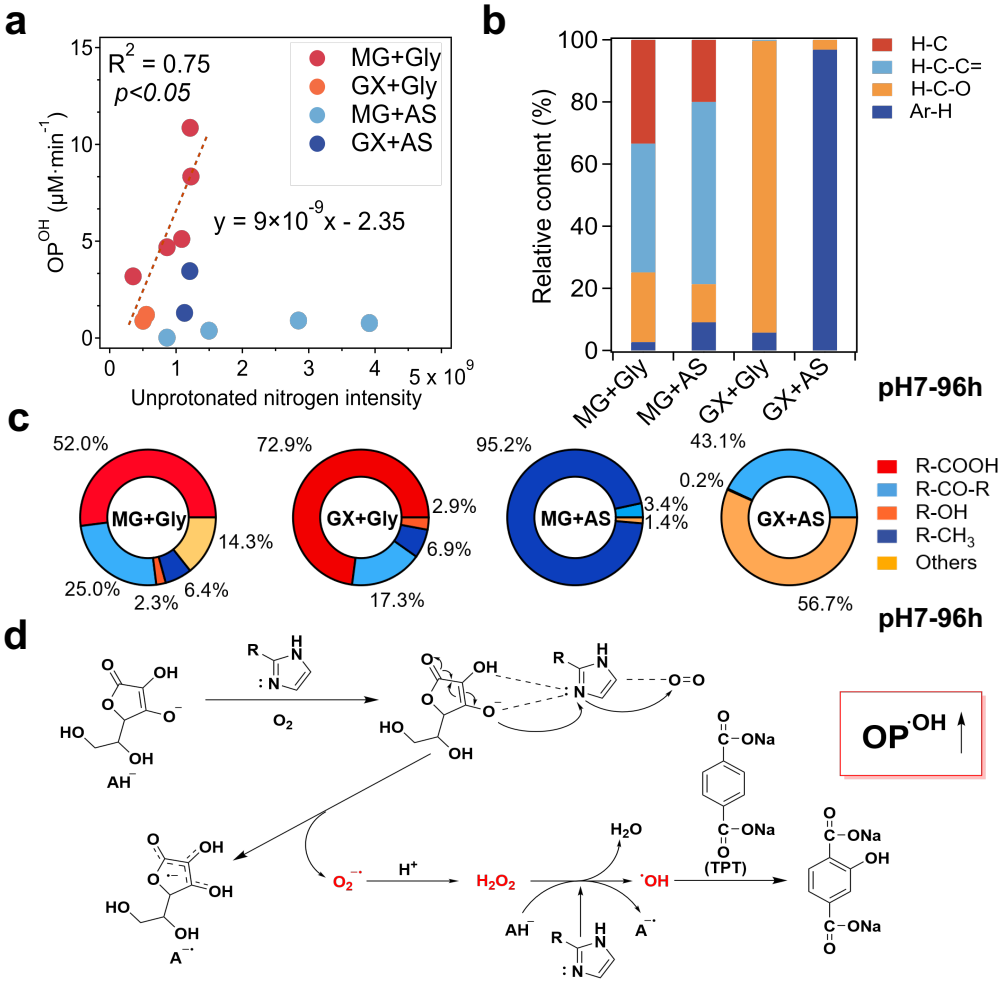

385 **Figure 7.** (a) The relationship between the signal intensities of N-heterocycles with unprotonated N-base identified in the four reaction systems and their corresponding OP^{OH}. (b) The relative contents of site-specific hydrogen atoms in the four reaction systems after 96 h of reaction under pH 7, as determined by NMR spectroscopy. (c) The peak area-weighted proportion of N-heterocycles with different side chains in the four reaction systems after 96 h of reaction under pH 7. (d) The proposed mechanism for N-heterocycle-mediated •OH generation in the presence
390 of ascorbic acid.

As shown in Figures 7c and S13, more than 35% of the side chains adjacent to the unprotonated N-bases in the N-heterocycles formed in the MG/GX+Gly systems contain carboxyl groups, while such structural features are absent in the other two systems. Carboxyl can decrease the electron density of the N-heterocycle and enhance the electron-

https://doi.org/10.5194/egusphere-2026-3809
Preprint. Discussion started: 8 July 2026

withdrawing property of the unprotonated N-base, thereby increasing its electron-transfer capability (Wieczorkiewicz et al., 2024). This structural effect may account for the high OP^{OH} in the MG+Gly system (Figure 3a). A strong positive correlation was observed between the intensities of N-heterocycles with adjacent carboxyl groups and OP^{OH} (Figure S14, $R^2 = 0.88$, $p < 0.05$), further supporting that these structural features contribute to the elevated OP^{OH} in the MG+Gly system. Although the GX+Gly system also forms N-heterocycles with carboxylated side chains adjacent to the unprotonated N-bases, the overall signal intensities of unprotonated N-base species are much lower, consistent with its weaker OP^{OH}. Moreover, in the GX+Gly system, the signal intensities of N-heterocycles with adjacent carboxyl groups determined by UHPLC-HRMS/MS are comparable at pH 5 and 7 after 96 h of reaction (Figure S15). These results indicate that the abundance of N-heterocycles with adjacent carboxyl groups is similar across these pH conditions, explaining the comparable OP^{OH} observed at different pH values in the GX+Gly system (Figure 3c).

In the GX+AS system, the side chains adjacent to the unprotonated N-bases mainly contain carbonyl and hydroxyl groups (Figures 7c and S13). These substituents can also enhance the electron-withdrawing property of the unprotonated N-bases, though generally to a much lesser extent than carboxyl groups (Contreras et al., 2005; Wei et al., 2020; Wieczorkiewicz et al., 2021). Furthermore, high aromaticity indices (1.74 and 1.75 for 48 h and 96 h of reaction at pH 7, respectively, Figure S16) derived from the LC-MS/MS data (the calculation of aromaticity index is illustrated in the Supporting Information) indicate the formation of highly aromatic products. The identification of several representative N-heterocycles with more than two rings is shown in Figure S17, and they have also been reported in prior work (Gan et al., 2024). NMR also reveals a substantially higher proportion of Ar-H compared with the other systems (Figures 7b and S18). These results consistently suggest that the N-heterocycles in the GX+AS system are dominated by polycyclic aromatic structures. Such species possess extended conjugated systems, which afford the unprotonated N-bases stronger

https://doi.org/10.5194/egusphere-2026-3809
Preprint. Discussion started: 8 July 2026

electron-transfer capabilities than those in monocyclic heterocycles (Maclagan et al., 2014). This structural advantage likely contributes to the substantial •OH formation in this system (Figure 3d).

By contrast, methyl group is the dominant substituent in the MG+AS system, with more than 70% of the side chains adjacent to the unprotonated N-bases carrying methyl groups (Figures 7c and S13). Methyl groups are electron-donating, increasing the electron density of the N-heterocycle and thereby weakening its electron-transfer capacity (Xie et al., 2020). In addition, low aromaticity indices (less than 0.67, Figure S16) based on the LC-MS/MS results and weak Ar-H signals in NMR spectra (Figure S18) are found in the MG+AS system across all analyzed conditions. These characteristics suppress the electron-transfer step and result in inefficient •OH formation, explaining the persistently low OP^{OH} observed for the MG+AS system (Figure 3b). A summary of the observed OP^{OH} trend, key molecular species, structural features, and proposed mechanistic links to OP^{OH} is provided in Table S4.

To further verify the ability of N-heterocycles to mediate •OH formation, we tested several model compounds using •OH production assay, including imidazole, 2-methylimidazole, imidazole-2-carboxaldehyde, and imidazol-2-carboxylic acid. All four compounds exhibit considerable OP^{OH}, reaching approximately 28%~45% of Cu^{2+} at equivalent concentration (Figure S19). In addition, imidazol-2-carboxylic acid exhibits higher OP^{OH} than imidazole, while imidazole-2-carboxaldehyde shows slightly higher OP^{OH} than imidazole. In contrast, 2-methylimidazole displays lower OP^{OH} than imidazole. These trends indicate that electron-withdrawing substituents, particularly carboxyl groups, enhance the electron-transfer capability of N-heterocycles with unprotonated nitrogen, while the electron-donating substituents (e.g., methyl groups) tend to weaken this capability. Collectively, these results demonstrate that N-heterocycles with unprotonated N-bases can promote •OH formation, and that their activity is modulated by substituent-dependent electronic effects.

https://doi.org/10.5194/egusphere-2026-3809
Preprint. Discussion started: 8 July 2026

Based on the collective evidence, we conclude that the N-heterocycles with unprotonated N-bases are the main contributors to the observed OP^{OH} across the four reaction systems. Their ability to mediate •OH formation in the presence of ascorbic acid appears analogous to the role of redox-active metals, which catalyze electron transfer from ascorbic acid to O_2 thereby driving H_2O_2 and •OH formation (Charrier and Anastasio, 2011; Vidrio et al., 2008; Fang et al., 2016; Shen and Anastasio, 2012; Lin and Yu, 2020). Accordingly, we propose the following mechanism for N-heterocycle-mediated •OH generation in the presence of ascorbic acid (Figure 7d): the unprotonated N atom forms a hydrogen bond with the hydroxyl group of ascorbate anion ($AScH^-$) and simultaneously activates O_2, enabling electron transfer from ascorbate to O_2 to generate superoxide and form the ascorbyl radical ($Asc^{\bullet-}$). The superoxide is subsequently protonated and converted to H_2O_2. In the final step, the unprotonated N atom again acts as an electron-transfer mediator, facilitating electron transfer between H_2O_2 and $AScH^-/Asc^{\bullet-}$, leading to H_2O_2 decomposition and generating •OH.

4. Conclusions and Implications

This study identifies a previously underappreciated pathway but likely widespread source of OP in atmospheric PM: the aqueous-phase reactions between α-dicarbonyls and reduced nitrogen species. α-Dicarbonyls such as glyoxal and methylglyoxal are among the most abundant and ubiquitous oxygenated volatile organic compounds in atmospheric aerosols (Zhang et al., 2022). Reduced nitrogen species, including ammonium and amines, are likewise common constituents of atmospheric aerosols originating from agricultural emissions, biomass burning, and secondary formation (Behera et al., 2013), making their aqueous-phase interactions with α-dicarbonyls atmospherically widespread and impactful. While these reactions are known to generate light-absorbing BrC, their contribution to aerosol OP has remained overlooked. Our results demonstrate that products from these reactions can exhibit substantial OP, establishing aqueous-phase chemistry as an important parallel pathway to gas-phase photochemistry in generating species that

https://doi.org/10.5194/egusphere-2026-3809
Preprint. Discussion started: 8 July 2026

promote ROS formation, particularly in atmospheric aqueous processing or during high-humidity haze episodes. The oxidative properties of these products are health-relevant, as they may generate ROS and contribute to oxidative stress, a key mechanism linking PM exposure to adverse respiratory and cardiovascular outcomes.

The OP of these products is strongly modulated by multiple factors, including precursor identity, solution pH, and reaction time, which together determine their ability to drive DTT oxidation and •OH formation. Among the reaction systems investigated, the MG+Gly system consistently exhibits the highest OP^{DTT} and OP^{OH}, suggesting the importance of methylglyoxal, a high-yield oxidation product of both biogenic and anthropogenic volatile organic compounds (Fu et al., 2008; Lim et al., 2005; Li et al., 2014), and amino acids in forming potent oxidants. While field measurements simultaneously determining MG and Gly in ambient particles are lacking, global modelling and observational studies have demonstrated the high abundance and ubiquity of MG, as well as its favorable partitioning into the particle phase (Fu et al., 2008; Hu et al., 2022). Furthermore, Gly is frequently reported as the most abundant free amino acid in ambient fine particles (Song et al., 2017; Zhu et al., 2020). These findings indicate that the MG+Gly reaction system is atmospherically relevant and warrants attention for its potential to form potent oxidants in ambient particles. Nevertheless, direct extrapolation of these laboratory findings to the real atmosphere should be made with caution, given fundamental differences between bulk solution reactions and authentic atmospheric aqueous-phase processes. The observed pH-dependence, with reactivity suppressed under an acidic condition (pH 3) and maximized under neutral to mildly acidic conditions (pH 5–7), implies that the OP of PM influenced by this chemistry will vary spatially and temporally with atmospheric acidity.

Our findings also show clear mechanistic distinctions between contributors to OP^{DTT} and OP^{OH}. Additionally, our findings highlight the key roles of N-heterocycles in generating ROS and contributing to the oxidative potential properties of atmospheric aerosols. CHO species, including conjugated carbonyls and quinone-like compounds enriched

https://doi.org/10.5194/egusphere-2026-3809
Preprint. Discussion started: 8 July 2026

in the MG+Gly system, primarily drive DTT oxidation. N-heterocycles with unprotonated N-bases, a major product class formed from α-dicarbonyls and reduced nitrogen species, can further enhance DTT activity through synergistic interactions with quinone intermediates. More importantly, these N-heterocycles are identified as the main contributors to •OH formation. The presence of electron-withdrawing substituents adjacent to the unprotonated N-bases substantially amplifies their electron-transfer capability, suggesting that the oxidative capacity of these molecules can increase as they age in the atmosphere. It is also worth mentioning that, while the combined use of DTT and •OH assays provides complementary insights into oxidative properties, the inclusion of additional assays (e.g., ascorbic acid assay) could offer a more comprehensive evaluation of OP (Zhu et al., 2020), and warrants future investigation.

The atmospheric relevance of this chemistry is underscored by the ubiquity of the precursors (α-dicarbonyls and reduced nitrogen) in atmospheric PM. Their co-occurrence under humid conditions creates favorable environments for the aqueous-phase reactions investigated here. These reactions represent a previously underappreciated and potentially widespread source of oxidatively active PM components. Beyond aqueous reactions, N-heterocycles with unprotonated N-bases are also emitted directly from biomass burning and can form through other gas- and particle-phase pathways (Wang et al., 2017; Laskin et al., 2015). Given that climate change is increasing the frequency and intensity of wildfires, nitrogen-containing organic compounds, including a substantial fraction of N-heterocycles, are expected to constitute a growing fraction of organic aerosols in the atmosphere (Zhong et al., 2024; Bhattarai et al., 2023; Li et al., 2025). Consequently, the aqueous-phase formation pathways elucidated in this work will likely become increasingly important for generating PM components that contribute to the oxidative properties of PM in regions affected by wildfire emissions and other biomass-burning activities.

Data availability

https://doi.org/10.5194/egusphere-2026-3809
Preprint. Discussion started: 8 July 2026

The data are available upon request to the corresponding author Fobang Liu (fobang.liu@xjtu.edu.cn) and Yuemei Han (yuemei.han@ieecas.cn).

Author contributions

FL and YP designed the research. YP, YW, XZ, XY, and YW carried out the experiments. FL, YH, CH, and TN supervised the study. FL and YP prepared the original manuscript with input from all the co-authors.

Competing interests

At least one of the (co-)authors is a member of the editorial board of Atmospheric Chemistry and Physics.

Disclaimer

Publisher's note: Copernicus Publications remains neutral with regard to jurisdictional claims made in the text, published maps, institutional affiliations, or any other geographical representation in this paper. While Copernicus Publications makes every effort to include appropriate place names, the final responsibility lies with the authors.

Acknowledgments

This work is supported by the National Natural Science Foundation of China (42475111).

References

Abrams, J. Y., Weber, R. J., Klein, M., Samat, S. E., Chang, H. H., Strickland, M. J., Verma, V., Fang, T., Bates, J. T., Mulholland, J. A., Russell, A. G., and Tolbert, P. E.: Associations between Ambient

https://doi.org/10.5194/egusphere-2026-3809
Preprint. Discussion started: 8 July 2026

Fine Particulate Oxidative Potential and Cardiorespiratory Emergency Department Visits, Environmental Health Perspectives, 125 http://doi.org/10.1289/ehp1545, 2017.

Atkinson, R. W., Samoli, E., Analitis, A., Fuller, G. W., Green, D. C., Anderson, H. R., Purdie, E., Dunster, C., Aitlhadj, L., Kelly, F. J., and Mudway, I. S.: Short-term associations between particle oxidative potential and daily mortality and hospital admissions in London, International Journal of Hygiene and Environmental Health, 219, 566-572 http://doi.org/10.1016/j.ijheh.2016.06.004, 2016.

Bates, J. T., Fang, T., Verma, V., Zeng, L., Weber, R. J., Tolbert, P. E., Abrams, J. Y., Sarnat, S. E., Klein, M., Mulholland, J. A., and Russell, A. G.: Review of Acellular Assays of Ambient Particulate Matter Oxidative Potential: Methods and Relationships with Composition, Sources, and Health Effects, Environ Sci Technol, 53, 4003-4019 http://doi.org/10.1021/acs.est.8b03430, 2019.

Bates, J. T., Weber, R. J., Abrams, J., Verma, V., Fang, T., Klein, M., Strickland, M. J., Sarnat, S. E., Chang, H. H., Mulholland, J. A., Tolbert, P. E., and Russell, A. G.: Reactive Oxygen Species Generation Linked to Sources of Atmospheric Particulate Matter and Cardiorespiratory Effects, Environmental Science & Technology, 49, 13605-13612 http://doi.org/10.1021/acs.est.5b02967, 2015.

Behera, S. N., Sharma, M., Aneja, V. P., and Balasubramanian, R.: Ammonia in the atmosphere: a review on emission sources, atmospheric chemistry and deposition on terrestrial bodies, Environmental Science and Pollution Research, 20, 8092-8131 http://doi.org/10.1007/s11356-013-2051-9, 2013.

Bhattarai, H., Wu, G., Zheng, X., Zhu, H., Gao, S., Zhang, Y.-L., Widory, D., Ram, K., Chen, X., Wan, X., Pei, Q., Pan, Y., Kang, S., and Cong, Z.: Wildfire-Derived Nitrogen Aerosols Threaten the Fragile Ecosystem in Himalayas and Tibetan Plateau, Environmental Science & Technology, 57, 9243-9251 http://doi.org/10.1021/acs.est.3c01541, 2023.

Burnett, R., Chen, H., Szyszkowicz, M., Fann, N., Hubbell, B., Pope, C. A., Apte, J. S., Brauer, M., Cohen, A., Weichenthal, S., Coggins, J., Di, Q., Brunekreef, B., Frostad, J., Lim, S. S., Kan, H., Walker, K. D., Thurston, G. D., Hayes, R. B., Lim, C. C., Turner, M. C., Jerrett, M., Krewski, D., Gapstur, S. M., Diver, W. R., Ostro, B., Goldberg, D., Crouse, D. L., Martin, R. V., Peters, P., Pinault, L., Tjepkema, M., van Donkelaar, A., Villeneuve, P. J., Miller, A. B., Yin, P., Zhou, M., Wang, L., Janssen, N. A. H., Marra, M., Atkinson, R. W., Tsang, H., Quoc Thach, T., Cannon, J. B., Allen, R. T., Hart, J. E., Laden, F., Cesaroni, G., Forastiere, F., Weinmayr, G., Jaensch, A., Nagel, G., Concin, H., and Spadaro, J. V.: Global estimates of mortality associated with long-term exposure to outdoor

https://doi.org/10.5194/egusphere-2026-3809
Preprint. Discussion started: 8 July 2026

fine particulate matter, Proceedings of the National Academy of Sciences, 115, 9592-9597 http://doi.org/10.1073/pnas.1803222115, 2018.

Campbell, S. J., Utinger, B., Barth, A., Paulson, S. E., and Kalberer, M.: Iron and Copper Alter the Oxidative Potential of Secondary Organic Aerosol: Insights from Online Measurements and Model Development, Environ Sci Technol, 57, 13546-13558 http://doi.org/10.1021/acs.est.3c01975, 2023.

Campbell, S. J., Utinger, B., Barth, A., Leni, Z., Zhang, Z. H., Resch, J., Li, K., Steimer, S. S., Banach, C., Gfeller, B., Wragg, F. P. H., Westwood, J., Wolfer, K., Bukowiecki, N., Ihalainen, M., Yli-Pirila, P., Somero, M., Kortelainen, M., Louhisalmi, J., Sklorz, M., Czech, H., di Bucchianico, S., Streibel, T., Delaval, M. N., Ruger, C., Baumlin, N., Salathe, M., Fang, Z., Pardo, M., D'Aronco, S., Giorio, C., Shi, Z., Harrison, R. M., Green, D. C., Kelly, F. J., Rudich, Y., Paulson, S. E., Sippula, O., Zimmermann, R., Geiser, M., and Kalberer, M.: Short-lived reactive components substantially contribute to particulate matter oxidative potential, Sci Adv, 11, eadp8100 http://doi.org/10.1126/sciadv.adp8100, 2025.

Charrier, J. G. and Anastasio, C.: Impacts of antioxidants on hydroxyl radical production from individual and mixed transition metals in a surrogate lung fluid, Atmospheric Environment, 45, 7555-7562 http://doi.org/10.1016/j.atmosenv.2010.12.021, 2011.

Charrier, J. G. and Anastasio, C.: On dithiothreitol (DTT) as a measure of oxidative potential for ambient particles: evidence for the importance of soluble transition metals, Atmospheric Chemistry and Physics, 12, 9321-9333 http://doi.org/10.5194/acp-12-9321-2012, 2012.

Charrier, J. G. and Anastasio, C.: Rates of Hydroxyl Radical Production from Transition Metals and Quinones in a Surrogate Lung Fluid, Environmental Science & Technology, 49, 9317-9325 http://doi.org/10.1021/acs.est.5b01606, 2015.

Chen, J. Y., Jiang, H., Chen, S. J., Cullen, C., Ahmed, C. M. S., and Lin, Y.-H.: Characterization of electrophilicity and oxidative potential of atmospheric carbonyls, Environmental Science: Processes & Impacts, 21, 856-866 http://doi.org/10.1039/c9em00033j, 2019a.

Chen, Q., Wang, M., Wang, Y., Zhang, L., Li, Y., and Han, Y.: Oxidative Potential of Water-Soluble Matter Associated with Chromophoric Substances in PM2.5 over Xi'an, China, Environmental Science & Technology, 53, 8574-8584 http://doi.org/10.1021/acs.est.9b01976, 2019b.

Cohen, A. J., Brauer, M., Burnett, R., Anderson, H. R., Frostad, J., Estep, K., Balakrishnan, K., Brunekreef, B., Dandona, L., Dandona, R., Feigin, V., Freedman, G., Hubbell, B., Jobling, A., Kan, H., Knibbs, L., Liu, Y., Martin, R., Morawska, L., Pope, C. A., Shin, H., Straif, K., Shaddick, G., Thomas, M., van Dingenen, R., van Donkelaar, A., Vos, T., Murray, C. J. L., and Forouzanfar, M. H.:

https://doi.org/10.5194/egusphere-2026-3809
Preprint. Discussion started: 8 July 2026

Estimates and 25-year trends of the global burden of disease attributable to ambient air pollution: an analysis of data from the Global Burden of Diseases Study 2015, The Lancet, 389, 1907-1918 http://doi.org/10.1016/s0140-6736(17)30505-6, 2017.

Contreras, R., Andrés, J., Domingo, L. R., Castillo, R., and Pérez, P.: Effect of electron-withdrawing substituents on the electrophilicity of carbonyl carbons, Tetrahedron, 61, 417-422 http://doi.org/10.1016/j.tet.2004.10.085, 2005.

Crobeddu, B., Aragao-Santiago, L., Bui, L.-C., Boland, S., and Baeza Squiban, A.: Oxidative potential of particulate matter 2.5 as predictive indicator of cellular stress, Environmental Pollution, 230, 125-133 http://doi.org/10.1016/j.envpol.2017.06.051, 2017.

Daellenbach, K. R., Uzu, G., Jiang, J., Cassagnes, L.-E., Leni, Z., Vlachou, A., Stefenelli, G., Canonaco, F., Weber, S., Segers, A., Kuenen, J. J. P., Schaap, M., Favez, O., Albinet, A., Aksoyoglu, S., Dommen, J., Baltensperger, U., Geiser, M., El Haddad, I., Jaffrezo, J.-L., and Prévôt, A. S. H.: Sources of particulate-matter air pollution and its oxidative potential in Europe, Nature, 587, 414-419 http://doi.org/10.1038/s41586-020-2902-8, 2020.

De Haan, D. O.: Aqueous Aerosol Processing of Glyoxal and Methylglyoxal: Recent Measurements of Uptake Coefficients, SOA Production, and Brown Carbon Formation, Acs Sym Ser, 1299, 149-167 http://doi.org/10.1021/bk-2018-1299.ch008, 2018.

De Haan, D. O., Corrigan, A. L., Tolbert, M. A., Jimenez, J. L., Wood, S. E., and Turley, J. J.: Secondary Organic Aerosol Formation by Self-Reactions of Methylglyoxal and Glyoxal in Evaporating Droplets, Environmental Science & Technology, 43, 8184-8190 http://doi.org/10.1021/es902152t, 2009.

De Haan, D. O., Tapavicza, E., Riva, M., Cui, T., Surratt, J. D., Smith, A. C., Jordan, M.-C., Nilakantan, S., Almodovar, M., Stewart, T. N., de Loera, A., De Haan, A. C., Cazaunau, M., Gratien, A., Pangui, E., and Doussin, J.-F.: Nitrogen-Containing, Light-Absorbing Oligomers Produced in Aerosol Particles Exposed to Methylglyoxal, Photolysis, and Cloud Cycling, Environmental Science & Technology, 52, 4061-4071 http://doi.org/10.1021/acs.est.7b06105, 2018.

Ditto, J. C., Joo, T., Slade, J. H., Shepson, P. B., Ng, N. L., and Gentner, D. R.: Nontargeted Tandem Mass Spectrometry Analysis Reveals Diversity and Variability in Aerosol Functional Groups across Multiple Sites, Seasons, and Times of Day, Environmental Science & Technology Letters, 7, 60-69 http://doi.org/10.1021/acs.estlett.9b00702, 2020.

Dou, J., Lin, P., Kuang, B.-Y., and Yu, J. Z.: Reactive Oxygen Species Production Mediated by Humic-like Substances in Atmospheric Aerosols: Enhancement Effects by Pyridine, Imidazole, and

https://doi.org/10.5194/egusphere-2026-3809
Preprint. Discussion started: 8 July 2026

Their Derivatives, Environmental Science & Technology, 49, 6457-6465 http://doi.org/10.1021/es5059378, 2015.

Dührkop, K., Fleischauer, M., Ludwig, M., Aksenov, A. A., Melnik, A. V., Meusel, M., Dorrestein, P. C., Rousu, J., and Böcker, S.: SIRIUS 4: a rapid tool for turning tandem mass spectra into metabolite structure information, Nature Methods, 16, 299-302 http://doi.org/10.1038/s41592-019-0344-8, 2019.

Ervens, B. and Volkamer, R.: Glyoxal processing by aerosol multiphase chemistry: towards a kinetic modeling framework of secondary organic aerosol formation in aqueous particles, Atmospheric Chemistry and Physics, 10, 8219-8244 http://doi.org/10.5194/acp-10-8219-2010, 2010.

Ervens, B., Turpin, B. J., and Weber, R. J.: Secondary organic aerosol formation in cloud droplets and aqueous particles (aqSOA): a review of laboratory, field and model studies, Atmospheric Chemistry and Physics, 11, 11069-11102 http://doi.org/10.5194/acp-11-11069-2011, 2011.

Fan, P., Xie, X.-H., Chen, C.-H., Peng, X., Zhang, P., Yang, C., and Wang, Y.-T.: Molecular Regulation Mechanisms and Interactions Between Reactive Oxygen Species and Mitophagy, DNA and Cell Biology, 38, 10-22 http://doi.org/10.1089/dna.2018.4348, 2019.

Fang, T., Lakey, P. S. J., Weber, R. J., and Shiraiwa, M.: Oxidative Potential of Particulate Matter and Generation of Reactive Oxygen Species in Epithelial Lining Fluid, Environmental Science & Technology, 53, 12784-12792 http://doi.org/10.1021/acs.est.9b03823, 2019.

Fang, T., Verma, V., Bates, J. T., Abrams, J., Klein, M., Strickland, M. J., Sarnat, S. E., Chang, H. H., Mulholland, J. A., Tolbert, P. E., Russell, A. G., and Weber, R. J.: Oxidative potential of ambient water-soluble PM2.5 in the southeastern United States: contrasts in sources and health associations between ascorbic acid (AA) and dithiothreitol (DTT) assays, Atmospheric Chemistry and Physics, 16, 3865-3879 http://doi.org/10.5194/acp-16-3865-2016, 2016.

Fu, T. M., Jacob, D. J., Wittrock, F., Burrows, J. P., Vrekoussis, M., and Henze, D. K.: Global budgets of atmospheric glyoxal and methylglyoxal, and implications for formation of secondary organic aerosols, Journal of Geophysical Research: Atmospheres, 113 http://doi.org/10.1029/2007jd009505, 2008.

Gan, Y., Lu, X., Chen, S., Jiang, X., Yang, S., Ma, X., Li, M., Yang, F., Shi, Y., and Wang, X.: Aqueous-phase formation of N-containing secondary organic compounds affected by the ionic strength, Journal of Environmental Sciences, 138, 88-101 http://doi.org/10.1016/j.jes.2023.03.003, 2024.

https://doi.org/10.5194/egusphere-2026-3809
Preprint. Discussion started: 8 July 2026

Georgopoulou, M. P., Florou, K., Matrali, A., Starida, G., Kaltsonoudis, C., Nenes, A., and Pandis, S. N.: Diurnal aging of biomass burning emissions: impacts on secondary organic aerosol formation and oxidative potential, Atmospheric Chemistry and Physics, 25, 15835-15855 http://doi.org/10.5194/acp-25-15835-2025, 2025.

Grace, D. N., Lugos, E. N., Ma, S., Griffith, D. R., Hendrickson, H. P., Woo, J. L., and Galloway, M. M.: Brown Carbon Formation Potential of the Biacetyl–Ammonium Sulfate Reaction System, ACS Earth and Space Chemistry, 4, 1104-1113 http://doi.org/10.1021/acsearthspacechem.0c00096, 2020.

Guin, P. S., Das, S., and Mandal, P. C.: Electrochemical Reduction of Quinones in Different Media: A Review, International Journal of Electrochemistry, 2011, 1-22 http://doi.org/10.4061/2011/816202, 2011.

Haan, D. O. D., Corrigan, A. L., Smith, K. W., Stroik, D. R., Turley, J. J., Lee, F. E., Tolbert, M. A., Jimenez, J. L., Cordova, K. E., and Ferrell, G. R.: Secondary Organic Aerosol-Forming Reactions of Glyoxal with Amino Acids, Environmental Science & Technology, 43, 2818-2824 http://doi.org/10.1021/es803534f, 2009.

Hawkins, L. N., Lemire, A. N., Galloway, M. M., Corrigan, A. L., Turley, J. J., Espelien, B. M., and De Haan, D. O.: Maillard Chemistry in Clouds and Aqueous Aerosol As a Source of Atmospheric Humic-Like Substances, Environ Sci Technol, 50, 7443-7452 http://doi.org/10.1021/acs.est.6b00909, 2016.

He, L. and Zhang, J.: Particulate matter (PM) oxidative potential: Measurement methods and links to PM physicochemical characteristics and health effects, Critical Reviews in Environmental Science and Technology, 53, 177-197 http://doi.org/10.1080/10643389.2022.2050148, 2022.

Hems, R. F., Schnitzler, E. G., Liu-Kang, C., Cappa, C. D., and Abbatt, J. P. D.: Aging of Atmospheric Brown Carbon Aerosol, Acs Earth and Space Chemistry, 5, 722-748 http://doi.org/10.1021/acsearthspacechem.0c00346, 2021.

Hodzic, A., Kasibhatla, P. S., Jo, D. S., Cappa, C. D., Jimenez, J. L., Madronich, S., and Park, R. J.: Rethinking the global secondary organic aerosol (SOA) budget: stronger production, faster removal, shorter lifetime, Atmospheric Chemistry and Physics, 16, 7917-7941 http://doi.org/10.5194/acp-16-7917-2016, 2016.

Hu, J., Chen, Z., Qin, X., and Dong, P.: Reversible and irreversible gas–particle partitioning of dicarbonyl compounds observed in the real atmosphere, Atmospheric Chemistry and Physics, 22, 6971-6987 http://doi.org/10.5194/acp-22-6971-2022, 2022.

https://doi.org/10.5194/egusphere-2026-3809
Preprint. Discussion started: 8 July 2026

Huang, R.-J., Yang, L., Cao, J., Chen, Y., Chen, Q., Li, Y., Duan, J., Zhu, C., Dai, W., Wang, K., Lin, C., Ni, H., Corbin, J. C., Wu, Y., Zhang, R., Tie, X., Hoffmann, T., O'Dowd, C., and Dusek, U.: Brown Carbon Aerosol in Urban Xi'an, Northwest China: The Composition and Light Absorption Properties, Environmental Science & Technology, 52, 6825-6833 http://doi.org/10.1021/acs.est.8b02386, 2018.

Huang, R.-J., Li, Y. J., Chen, Q., Zhang, Y., Lin, C., Chan, C. K., Yu, J. Z., de Gouw, J., Tong, S., Jiang, J., Wang, W., Ding, X., Wang, X., Ge, M., Zhou, W., Worsnop, D., Boy, M., Bilde, M., Dusek, U., Carlton, A. G., Hoffmann, T., McNeill, V. F., and Glasius, M.: Secondary organic aerosol in urban China: A distinct chemical regime for air pollution studies, Science, 389 http://doi.org/10.1126/science.adq2840, 2025.

Jiang, H. and Jang, M.: Dynamic Oxidative Potential of Atmospheric Organic Aerosol under Ambient Sunlight, Environmental Science & Technology, 52, 7496-7504 http://doi.org/10.1021/acs.est.8b00148, 2018.

Jiang, H., Ahmed, C. M. S., Canchola, A., Chen, J. Y., and Lin, Y.-H.: Use of Dithiothreitol Assay to Evaluate the Oxidative Potential of Atmospheric Aerosols, Atmosphere, 10 http://doi.org/10.3390/atmos10100571, 2019.

Jiang, H., Ahmed, C. M. S., Zhao, Z., Chen, J. Y., Zhang, H., Canchola, A., and Lin, Y.-H.: Role of functional groups in reaction kinetics of dithiothreitol with secondary organic aerosols, Environmental Pollution, 263 http://doi.org/10.1016/j.envpol.2020.114402, 2020.

Jimenez, J. L., Canagaratna, M. R., Donahue, N. M., Prevot, A. S. H., Zhang, Q., Kroll, J. H., DeCarlo, P. F., Allan, J. D., Coe, H., Ng, N. L., Aiken, A. C., Docherty, K. S., Ulbrich, I. M., Grieshop, A. P., Robinson, A. L., Duplissy, J., Smith, J. D., Wilson, K. R., Lanz, V. A., Hueglin, C., Sun, Y. L., Tian, J., Laaksonen, A., Raatikainen, T., Rautiainen, J., Vaattovaara, P., Ehn, M., Kulmala, M., Tomlinson, J. M., Collins, D. R., Cubison, M. J., Dunlea, J., Huffman, J. A., Onasch, T. B., Alfarra, M. R., Williams, P. I., Bower, K., Kondo, Y., Schneider, J., Drewnick, F., Borrmann, S., Weimer, S., Demerjian, K., Salcedo, D., Cottrell, L., Griffin, R., Takami, A., Miyoshi, T., Hatakeyama, S., Shimono, A., Sun, J. Y., Zhang, Y. M., Dzepina, K., Kimmel, J. R., Sueper, D., Jayne, J. T., Herndon, S. C., Trimborn, A. M., Williams, L. R., Wood, E. C., Middlebrook, A. M., Kolb, C. E., Baltensperger, U., and Worsnop, D. R.: Evolution of Organic Aerosols in the Atmosphere, Science, 326, 1525-1529 http://doi.org/10.1126/science.1180353, 2009.

https://doi.org/10.5194/egusphere-2026-3809
Preprint. Discussion started: 8 July 2026

Kampf, C. J., Filippi, A., Zuth, C., Hoffmann, T., and Opatz, T.: Secondary brown carbon formation via the dicarbonyl imine pathway: nitrogen heterocycle formation and synergistic effects, Physical Chemistry Chemical Physics, 18, 18353-18364 http://doi.org/10.1039/c6cp03029g, 2016.

Kawamura, K., Okuzawa, K., Aggarwal, S. G., Irie, H., Kanaya, Y., and Wang, Z.: Determination of gaseous and particulate carbonyls (glycolaldehyde, hydroxyacetone, glyoxal, methylglyoxal, nonanal and decanal) in the atmosphere at Mt. Tai, Atmospheric Chemistry and Physics, 13, 5369-5380 http://doi.org/10.5194/acp-13-5369-2013, 2013.

Kipp, B. H., Faraj, C., Li, G., and Njus, D.: Imidazole facilitates electron transfer from organic reductants, Bioelectrochemistry, 64, 7-13 http://doi.org/10.1016/j.bioelechem.2003.12.010, 2004.

Kuang, Y., Guo, Y., Chai, J., Shang, J., Zhu, J., Stevanovic, S., and Ristovski, Z.: Comparison of light absorption and oxidative potential of biodiesel/diesel and chemicals/diesel blends soot particles, Journal of Environmental Sciences, 87, 184-193 http://doi.org/10.1016/j.jes.2019.06.014, 2020.

Lai, R. W. S., Qiu, T., Zhang, X., Wang, Y., Hao, T., Ge, X., Du, L., Tang, M., Hoi, K. I., Mok, K. M., and Li, Y. J.: Deciphering the key drivers of oxidative potential during ammonium nitrate-mediated aqueous-phase photoreaction of methoxyphenols, Atmospheric Environment, 340 http://doi.org/10.1016/j.atmosenv.2024.120895, 2025.

Lakey, P. S. J., Berkemeier, T., Tong, H., Arangio, A. M., Lucas, K., Pöschl, U., and Shiraiwa, M.: Chemical exposure-response relationship between air pollutants and reactive oxygen species in the human respiratory tract, Scientific Reports, 6 http://doi.org/10.1038/srep32916, 2016.

Laskin, A., Laskin, J., and Nizkorodov, S. A.: Chemistry of Atmospheric Brown Carbon, Chemical Reviews, 115, 4335-4382 http://doi.org/10.1021/cr5006167, 2015.

Lei, R., Sha, Y., Meng, H., Huang, Y., Ye, J., Huang, D. D., Zhang, Y., Wu, Y., Li, Y., and Ge, X.: Aqueous phase photolysis of 4-nitrocatechol: Reaction kinetics, evolutions of chemical composition, light absorption and oxidation potential, Atmospheric Environment, 343 http://doi.org/10.1016/j.atmosenv.2024.120981, 2025.

Lelieveld, J., Evans, J. S., Fnais, M., Giannadaki, D., and Pozzer, A.: The contribution of outdoor air pollution sources to premature mortality on a global scale, Nature, 525, 367-371 http://doi.org/10.1038/nature15371, 2015.

Li, N., Sioutas, C., Cho, A., Schmitz, D., Misra, C., Sempf, J., Wang, M., Oberley, T., Froines, J., and Nel, A.: Ultrafine particulate pollutants induce oxidative stress and mitochondrial damage, Environmental Health Perspectives, 111, 455-460 http://doi.org/10.1289/ehp.6000, 2003.

https://doi.org/10.5194/egusphere-2026-3809
Preprint. Discussion started: 8 July 2026

Li, R., Han, Y., Wang, L., Shang, Y., and Chen, Y.: Differences in oxidative potential of black carbon from three combustion emission sources in China, Journal of Environmental Management, 240, 57-65 http://doi.org/10.1016/j.jenvman.2019.03.070, 2019.

Li, X., Kuang, X. M., Yan, C., Ma, S., Paulson, S. E., Zhu, T., Zhang, Y., and Zheng, M.: Oxidative Potential by PM2.5 in the North China Plain: Generation of Hydroxyl Radical, Environmental Science & Technology, 53, 512-520 http://doi.org/10.1021/acs.est.8b05253, 2018.

Li, X., Rohrer, F., Brauers, T., Hofzumahaus, A., Lu, K., Shao, M., Zhang, Y. H., and Wahner, A.: Modeling of HCHO and CHOCHO at a semi-rural site in southern China during the PRIDE-PRD2006 campaign, Atmospheric Chemistry and Physics, 14, 12291-12305 http://doi.org/10.5194/acp-14-12291-2014, 2014.

Li, Y., Fu, T.-M., Yu, J. Z., Zhang, A., Yu, X., Ye, J., Zhu, L., Shen, H., Wang, C., Yang, X., Tao, S., Chen, Q., Li, Y., Li, L., Che, H., and Heald, C. L.: Nitrogen dominates global atmospheric organic aerosol absorption, Science, 387, 989-995 http://doi.org/10.1126/science.adr4473, 2025.

Lim, H.-J., Carlton, A. G., and Turpin, B. J.: Isoprene Forms Secondary Organic Aerosol through Cloud Processing: Model Simulations, Environmental Science & Technology, 39, 4441-4446 http://doi.org/10.1021/es048039h, 2005.

Lin, M. and Yu, J. Z.: Assessment of Interactions between Transition Metals and Atmospheric Organics: Ascorbic Acid Depletion and Hydroxyl Radical Formation in Organic-Metal Mixtures, Environmental Science & Technology, 54, 1431-1442 http://doi.org/10.1021/acs.est.9b07478, 2020.

Liu, F., Xu, T., Ng, N. L., and Lu, H.: Linking Cell Health and Reactive Oxygen Species from Secondary Organic Aerosols Exposure, Environmental Science & Technology, 57, 1039-1048 http://doi.org/10.1021/acs.est.2c05171, 2022.

Liu, F., Joo, T., Ditto, J. C., Saavedra, M. G., Takeuchi, M., Boris, A. J., Yang, Y., Weber, R. J., Dillner, A. M., Gentner, D. R., and Ng, N. L.: Oxidized and Unsaturated: Key Organic Aerosol Traits Associated with Cellular Reactive Oxygen Species Production in the Southeastern United States, Environmental Science & Technology, 57, 14150-14161 http://doi.org/10.1021/acs.est.3c03641, 2023.

Liu, F., Yang, X., Xu, W., Verma, V., Wang, Z., Chen, C., He, Y., Yang, L., Yang, Y., Sun, Y., and He, C.: Resolving Organic Aerosol Components Contributing to the Oxidative Potential of PM2.5 in the North China Plain, Journal of Geophysical Research: Atmospheres, 129 http://doi.org/10.1029/2024jd040840, 2024.

https://doi.org/10.5194/egusphere-2026-3809
Preprint. Discussion started: 8 July 2026

Liu, Y. and Chan, C. K.: The oxidative potential of fresh and aged elemental carbon-containing airborne particles: a review, Environmental Science: Processes & Impacts, 24, 525-546 http://doi.org/10.1039/d1em00497b, 2022.

Maclagan, R. G. A. R., Gronert, S., and Meot-Ner, M.: Protonated Polycyclic Aromatic Nitrogen Heterocyclics: Proton Affinities, Polarizabilities, and Atomic and Ring Charges of 1–5-Ring Ions, The Journal of Physical Chemistry A, 119, 127-139 http://doi.org/10.1021/jp5069939, 2014.

Melvin, M. S., Avery, K. C., Ballentine, R. M., Flora, J. W., Gardner, W., Karles, G. D., Pithawalla, Y. B., Smith, D. C., Ehman, K. D., and Wagner, K. A.: Formation of Diacetyl and Other α-Dicarbonyl Compounds during the Generation of E-Vapor Product Aerosols, ACS Omega, 5, 17565-17575 http://doi.org/10.1021/acsomega.0c02018, 2020.

Mitsuishi, K., Iwasaki, M., Takeuchi, M., Okochi, H., Kato, S., Ohira, S.-I., and Toda, K.: Diurnal Variations in Partitioning of Atmospheric Glyoxal and Methylglyoxal between Gas and Particles at the Ground Level and in the Free Troposphere, ACS Earth and Space Chemistry, 2, 915-924 http://doi.org/10.1021/acsearthspacechem.8b00037, 2018.

Ng, N. L., Canagaratna, M. R., Zhang, Q., Jimenez, J. L., Tian, J., Ulbrich, I. M., Kroll, J. H., Docherty, K. S., Chhabra, P. S., Bahreini, R., Murphy, S. M., Seinfeld, J. H., Hildebrandt, L., Donahue, N. M., DeCarlo, P. F., Lanz, V. A., Prévôt, A. S. H., Dinar, E., Rudich, Y., and Worsnop, D. R.: Organic aerosol components observed in Northern Hemispheric datasets from Aerosol Mass Spectrometry, Atmospheric Chemistry and Physics, 10, 4625-4641 http://doi.org/10.5194/acp-10-4625-2010, 2010.

Pluskal, T., Castillo, S., Villar-Briones, A., and Oresic, M.: MZmine 2: Modular framework for processing, visualizing, and analyzing mass spectrometry-based molecular profile data, Bmc Bioinformatics, 11 http://doi.org/Artn 395
10.1186/1471-2105-11-395, 2010.

Powelson, M. H., Espelien, B. M., Hawkins, L. N., Galloway, M. M., and De Haan, D. O.: Brown Carbon Formation by Aqueous-Phase Carbonyl Compound Reactions with Amines and Ammonium Sulfate, Environmental Science & Technology, 48, 985-993 http://doi.org/10.1021/es4038325, 2013.

Pripis-Nicolau, L., de Revel, G., Bertrand, A., and Maujean, A.: Formation of Flavor Components by the Reaction of Amino Acid and Carbonyl Compounds in Mild Conditions, Journal of Agricultural and Food Chemistry, 48, 3761-3766 http://doi.org/10.1021/jf991024w, 2000.

Pye, H. O. T., Nenes, A., Alexander, B., Ault, A. P., Barth, M. C., Clegg, S. L., Collett Jr, J. L., Fahey, K. M., Hennigan, C. J., Herrmann, H., Kanakidou, M., Kelly, J. T., Ku, I. T., McNeill, V. F., Riemer,

https://doi.org/10.5194/egusphere-2026-3809
Preprint. Discussion started: 8 July 2026

N., Schaefer, T., Shi, G., Tilgner, A., Walker, J. T., Wang, T., Weber, R., Xing, J., Zaveri, R. A., and Zuend, A.: The acidity of atmospheric particles and clouds, Atmospheric Chemistry and Physics, 20, 4809-4888 http://doi.org/10.5194/acp-20-4809-2020, 2020.

Rodriguez, A. A., de Loera, A., Powelson, M. H., Galloway, M. M., and De Haan, D. O.: Formaldehyde and Acetaldehyde Increase Aqueous-Phase Production of Imidazoles in Methylglyoxal/Amine Mixtures: Quantifying a Secondary Organic Aerosol Formation Mechanism, Environmental Science & Technology Letters, 4, 234-239 http://doi.org/10.1021/acs.estlett.7b00129, 2017.

Saffari, A., Daher, N., Shafer, M. M., Schauer, J. J., and Sioutas, C.: Global Perspective on the Oxidative Potential of Airborne Particulate Matter: A Synthesis of Research Findings, Environmental Science & Technology, 48, 7576-7583 http://doi.org/10.1021/es500937x, 2014.

Salana, S., Yu, H., Dai, Z., Subramanian, P. S. G., Puthussery, J. V., Wang, Y., Singh, A., Pope, F. D., Leiva G, M. A., Rastogi, N., Tripathi, S. N., Weber, R. J., and Verma, V.: Inter-continental variability in the relationship of oxidative potential and cytotoxicity with PM2.5 mass, Nature Communications, 15 http://doi.org/10.1038/s41467-024-49649-4, 2024.

Sedehi, N., Takano, H., Blasic, V. A., Sullivan, K. A., and De Haan, D. O.: Temperature- and pH-dependent aqueous-phase kinetics of the reactions of glyoxal and methylglyoxal with atmospheric amines and ammonium sulfate, Atmospheric Environment, 77, 656-663 http://doi.org/10.1016/j.atmosenv.2013.05.070, 2013.

Shen, H. and Anastasio, C.: A comparison of hydroxyl radical and hydrogen peroxide generation in ambient particle extracts and laboratory metal solutions, Atmospheric Environment, 46, 665-668 http://doi.org/10.1016/j.atmosenv.2011.10.006, 2012.

Shen, J., Taghvaee, S., La, C., Oroumiyeh, F., Liu, J., Jerrett, M., Weichenthal, S., Del Rosario, I., Shafer, M. M., Ritz, B., Zhu, Y., and Paulson, S. E.: Aerosol Oxidative Potential in the Greater Los Angeles Area: Source Apportionment and Associations with Socioeconomic Position, Environmental Science & Technology, 56, 17795-17804 http://doi.org/10.1021/acs.est.2c02788, 2022.

Siemens, K., Morales, A., He, Q., Li, C., Hettiyadura, A. P. S., Rudich, Y., and Laskin, A.: Molecular Analysis of Secondary Brown Carbon Produced from the Photooxidation of Naphthalene, Environmental Science & Technology, 56, 3340-3353 http://doi.org/10.1021/acs.est.1c03135, 2022.

Song, T., Wang, S., Zhang, Y., Song, J., Liu, F., Fu, P., Shiraiwa, M., Xie, Z., Yue, D., Zhong, L., Zheng, J., and Lai, S.: Proteins and Amino Acids in Fine Particulate Matter in Rural Guangzhou,

https://doi.org/10.5194/egusphere-2026-3809
Preprint. Discussion started: 8 July 2026

Southern China: Seasonal Cycles, Sources, and Atmospheric Processes, Environ Sci Technol, 51, 6773-6781 http://doi.org/10.1021/acs.est.7b00987, 2017.

Strak, M., Janssen, N. A. H., Godri, K. J., Gosens, I., Mudway, I. S., Cassee, F. R., Lebret, E., Kelly, F. J., Harrison, R. M., Brunekreef, B., Steenhof, M., and Hoek, G.: Respiratory Health Effects of Airborne Particulate Matter: The Role of Particle Size, Composition, and Oxidative Potential—The RAPTES Project, Environmental Health Perspectives, 120, 1183-1189 http://doi.org/10.1289/ehp.1104389, 2012.

Tang, S., Li, F., Lv, J., Liu, L., Wu, G., Wang, Y., Yu, W., Wang, Y., and Jiang, G.: Unexpected molecular diversity of brown carbon formed by Maillard-like reactions in aqueous aerosols, Chemical Science, 13, 8401-8411 http://doi.org/10.1039/d2sc02857c, 2022.

Tessier, F. J., Monnier, V. M., Sayre, L. M., and Kornfield, J. A.: Triosidines: novel Maillard reaction products and cross-links from the reaction of triose sugars with lysine and arginine residues, Biochemical Journal, 369, 705-719 http://doi.org/10.1042/bj20020668, 2003.

Tilgner, A., Schaefer, T., Alexander, B., Barth, M., Collett Jr, J. L., Fahey, K. M., Nenes, A., Pye, H. O. T., Herrmann, H., and McNeill, V. F.: Acidity and the multiphase chemistry of atmospheric aqueous particles and clouds, Atmospheric Chemistry and Physics, 21, 13483-13536 http://doi.org/10.5194/acp-21-13483-2021, 2021.

Trainic, M., Abo Riziq, A., Lavi, A., and Rudich, Y.: Role of Interfacial Water in the Heterogeneous Uptake of Glyoxal by Mixed Glycine and Ammonium Sulfate Aerosols, The Journal of Physical Chemistry A, 116, 5948-5957 http://doi.org/10.1021/jp2104837, 2012.

Tuet, W. Y., Chen, Y., Xu, L., Fok, S., Gao, D., Weber, R. J., and Ng, N. L.: Chemical oxidative potential of secondary organic aerosol (SOA) generated from the photooxidation of biogenic and anthropogenic volatile organic compounds, Atmospheric Chemistry and Physics, 17, 839-853 http://doi.org/10.5194/acp-17-839-2017, 2017.

Twerdok, L. E., Rembish, S. J., and Trush, M. A.: Studies with 1,2-dithiole-3-thione as a chemoprotector of hydroquinone-induced toxicity to DBA/2-derived bone marrow stromal cells, Environmental Health Perspectives, 101, 172-177 http://doi.org/10.1289/ehp.93101172, 1993.

Verma, V., Wang, Y., El-Afifi, R., Fang, T., Rowland, J., Russell, A. G., and Weber, R. J.: Fractionating ambient humic-like substances (HULIS) for their reactive oxygen species activity – Assessing the importance of quinones and atmospheric aging, Atmospheric Environment, 120, 351-359 http://doi.org/10.1016/j.atmosenv.2015.09.010, 2015.

https://doi.org/10.5194/egusphere-2026-3809
Preprint. Discussion started: 8 July 2026

Vidrio, E., Jung, H., and Anastasio, C.: Generation of hydroxyl radicals from dissolved transition metals in surrogate lung fluid solutions, Atmospheric Environment, 42, 4369-4379 http://doi.org/10.1016/j.atmosenv.2008.01.004, 2008.

Wang, J., Ye, J., Zhang, Q., Zhao, J., Wu, Y., Li, J., Liu, D., Li, W., Zhang, Y., Wu, C., Xie, C., Qin, Y., Lei, Y., Huang, X., Guo, J., Liu, P., Fu, P., Li, Y., Lee, H. C., Choi, H., Zhang, J., Liao, H., Chen, M., Sun, Y., Ge, X., Martin, S. T., and Jacob, D. J.: Aqueous production of secondary organic aerosol from fossil-fuel emissions in winter Beijing haze, Proceedings of the National Academy of Sciences, 118 http://doi.org/10.1073/pnas.2022179118, 2021.

Wang, S., Ye, J., Soong, R., Wu, B., Yu, L., Simpson, A. J., and Chan, A. W. H.: Relationship between chemical composition and oxidative potential of secondary organic aerosol from polycyclic aromatic hydrocarbons, Atmospheric Chemistry and Physics, 18, 3987-4003 http://doi.org/10.5194/acp-18-3987-2018, 2018.

Wang, Y. and Ho, C.-T.: Formation of 2,5-Dimethyl-4-hydroxy-3(2H)-furanone through Methylglyoxal: A Maillard Reaction Intermediate, Journal of Agricultural and Food Chemistry, 56, 7405-7409 http://doi.org/10.1021/jf8012025, 2008.

Wang, Y., Hu, M., Lin, P., Guo, Q., Wu, Z., Li, M., Zeng, L., Song, Y., Zeng, L., Wu, Y., Guo, S., Huang, X., and He, L.: Molecular Characterization of Nitrogen-Containing Organic Compounds in Humic-like Substances Emitted from Straw Residue Burning, Environmental Science & Technology, 51, 5951-5961 http://doi.org/10.1021/acs.est.7b00248, 2017.

Wei, J., Fang, T., and Shiraiwa, M.: Effects of Acidity on Reactive Oxygen Species Formation from Secondary Organic Aerosols, ACS Environmental Au, 2, 336-345 http://doi.org/10.1021/acsenvironau.2c00018, 2022.

Wei, Z., Liu, H., Yu, L., Xiao, S., Hou, Y., and Chen, X.: Delocalized aromatic molecules with matched electron-donating and electron-withdrawing groups enhancing insulating performance of polyethylene blends, Journal of Applied Polymer Science, 137 http://doi.org/10.1002/app.49185, 2020.

Wieczorkiewicz, P. A., Krygowski, T. M., and Szatylowicz, H.: Substituent effects and electron delocalization in five-membered N-heterocycles, Physical Chemistry Chemical Physics, 26, 19398-19410 http://doi.org/10.1039/d4cp01709a, 2024.

Wieczorkiewicz, P. A., Szatylowicz, H., and Krygowski, T. M.: Energetic and Geometric Characteristics of the Substituents: Part 2: The Case of NO2, Cl, and NH2 Groups in Their Mono-

https://doi.org/10.5194/egusphere-2026-3809
Preprint. Discussion started: 8 July 2026

Substituted Derivatives of Simple Nitrogen Heterocycles, Molecules, 26 http://doi.org/10.3390/molecules26216543, 2021.

Wong, J. P. S., Tsagkaraki, M., Tsiodra, I., Mihalopoulos, N., Violaki, K., Kanakidou, M., Sciare, J., Nenes, A., and Weber, R. J.: Effects of Atmospheric Processing on the Oxidative Potential of Biomass Burning Organic Aerosols, Environmental Science & Technology, 53, 6747-6756 http://doi.org/10.1021/acs.est.9b01034, 2019.

Xiao, B., Wang, G., Li, Z., Li, R., Liang, C., Wang, H., Zhang, S., Wu, C., Li, R., Zhang, F., Zhang, R., Wu, Y., and Zhang, L.: High Contribution of Secondary Formation to Brown Carbon in China Humid Haze: Enhancing Role of Ammonia and Amines, Environmental Science & Technology http://doi.org/10.1021/acs.est.5c13436, 2025.

Xie, C., Hu, X., Guan, Z., Li, X., Zhao, F., Song, Y., Li, Y., Li, X., Wang, N., and Huang, C.: Tuning the Properties of Graphdiyne by Introducing Electron-Withdrawing/Donating Groups, Angewandte Chemie International Edition, 59, 13542-13546 http://doi.org/10.1002/anie.202004454, 2020.

Xing, H. and Yaylayan, V.: Mechanochemistry of Strecker degradation: Interaction of glyoxal with amino acids, Food Chemistry, 439 http://doi.org/10.1016/j.foodchem.2023.138071, 2024.

Xiong, Q., Yu, H., Wang, R., Wei, J., and Verma, V.: Rethinking Dithiothreitol-Based Particulate Matter Oxidative Potential: Measuring Dithiothreitol Consumption versus Reactive Oxygen Species Generation, Environ Sci Technol, 51, 6507-6514 http://doi.org/10.1021/acs.est.7b01272, 2017.

Yang, A., Janssen, N. A. H., Brunekreef, B., Cassee, F. R., Hoek, G., and Gehring, U.: Children's respiratory health and oxidative potential of PM2.5: the PIAMA birth cohort study, Occupational and Environmental Medicine, 73, 154-160 http://doi.org/10.1136/oemed-2015-103175, 2016.

Yang, L., Huang, R.-J., Yuan, W., Huang, D. D., and Huang, C.: pH-Dependent Aqueous-Phase Brown Carbon Formation: Rate Constants and Implications for Solar Absorption and Atmospheric Photochemistry, Environmental Science & Technology, 58, 1236-1243 http://doi.org/10.1021/acs.est.3c07631, 2024a.

Yang, L., Huang, R.-J., Shen, J., Wang, T., Gong, Y., Yuan, W., Liu, Y., Huang, H., You, Q., Huang, D. D., and Huang, C.: New Insights into the Brown Carbon Chromophores and Formation Pathways for Aqueous Reactions of α-Dicarbonyls with Amines and Ammonium, Environmental Science & Technology, 57, 12351-12361 http://doi.org/10.1021/acs.est.3c04133, 2023.

Yang, X., Liu, F., Yang, S., Yang, Y., Wang, Y., Li, J., Zhao, M., Wang, Z., Wang, K., He, C., and Tong, H.: Atmospheric evolution of environmentally persistent free radicals in the rural North China

https://doi.org/10.5194/egusphere-2026-3809
Preprint. Discussion started: 8 July 2026

Plain: effects on water solubility and PM2.5 oxidative potential, Atmospheric Chemistry and Physics, 24, 11029-11043 http://doi.org/10.5194/acp-24-11029-2024, 2024b.

Yu, G., Bayer, A. R., Galloway, M. M., Korshavn, K. J., Fry, C. G., and Keutsch, F. N.: Glyoxal in aqueous ammonium sulfate solutions: products, kinetics and hydration effects, Environ Sci Technol, 45, 6336-6342 http://doi.org/10.1021/es200989n, 2011.

Yue, Y., Chen, H., Setyan, A., Elser, M., Dietrich, M., Li, J., Zhang, T., Zhang, X., Zheng, Y., Wang, J., and Yao, M.: Size-Resolved Endotoxin and Oxidative Potential of Ambient Particles in Beijing and Zürich, Environmental Science & Technology, 52, 6816-6824 http://doi.org/10.1021/acs.est.8b01167, 2018.

Zhang, Q., Wang, Y., Xiao, Q., Geng, G., Davis, S. J., Liu, X., Yang, J., Liu, J., Huang, W., He, C., Luo, B., Martin, R. V., Brauer, M., Randerson, J. T., and He, K.: Long-range PM2.5 pollution and health impacts from the 2023 Canadian wildfires, Nature, 645, 672-678 http://doi.org/10.1038/s41586-025-09482-1, 2025.

Zhang, Y., He, L., Sun, X., Ventura, O. N., and Herrmann, H.: Theoretical Investigation on the Oligomerization of Methylglyoxal and Glyoxal in Aqueous Atmospheric Aerosol Particles, ACS Earth and Space Chemistry, 6, 1031-1043 http://doi.org/10.1021/acsearthspacechem.1c00422, 2022.

Zhong, S., Liu, R., Yue, S., Wang, P., Zhang, Q., Ma, C., Deng, J., Qi, Y., Zhu, J., Liu, C.-Q., Kawamura, K., and Fu, P.: Peatland Wildfires Enhance Nitrogen-Containing Organic Compounds in Marine Aerosols over the Western Pacific, Environmental Science & Technology, 58, 10991-11002 http://doi.org/10.1021/acs.est.3c10125, 2024.

Zhu, R. g., Xiao, H. Y., Zhu, Y., Wen, Z., Fang, X., and Pan, Y.: Sources and Transformation Processes of Proteinaceous Matter and Free Amino Acids in PM2.5, Journal of Geophysical Research: Atmospheres, 125 http://doi.org/10.1029/2020jd032375, 2020.

https://doi.org/10.5194/egusphere-2026-3809
Preprint. Discussion started: 8 July 2026

TOC